Egypt. J. Agron. **Vol. 47**, No. 4, pp: 963 - 1003 (2025)

Egyptian Journal of Agronomy
http://agro.journals.ekb.eg/

Identifying The Best Systems for Managing Saline Water in Arid Regions to Improve Productivity, Water Productivity, and Citrus Quality

Mohamed M. Mahmoud[1,2*], Mohamed E. Abuarab[1*], Ayman Shaban[3] and **Elsayed Youssief Ghoniem[2]**

[1] *Agricultural Engineering Department, Faculty of Agriculture, Cairo University, PO box 12613 Giza, Egypt*

[2] *Basic and Applied Agricultural Sciences Department, Higher Institute of Agricultural Cooperation, Cairo, Egypt*

[3] *Fruit Department, Faculty of Agriculture, Cairo University, PO box 12613 Giza, Egypt*

THE RESEARCH focused on the sustainable management of irrigation water for orange farming in sandy soils with varying salinity levels, aiming to enhance the utilization of sustainable ecosystems while maximizing farmers' economic benefits. Field trials were conducted over two consecutive growing seasons, specifically from 2023 to 2025, utilizing six different irrigation techniques: T-tape GR drippers, online drippers, online PC drippers, mist sprayers, the Root Zone Watering System (RZWS), and bubblers. In the second growing season, the T-tape (GR) method achieved the highest yield of 27.54 ton ha^{-1}, while both the Bubbler and online PC dripper treatments yielded 27.54 ton $ha^{-1}$and 24.06 ton ha^{-1}, respectively. The mist sprayer produced the lowest yield at 18.09 ton ha^{-1}. In terms of irrigation water productivity (IWP), the T-tape (GR) recorded an IWP of 6.08 kg m^{-3} in the first growing season, closely followed by the online PC dripper at 5.37 kg m^{-3}. Conversely, the RZWS demonstrated the lowest IWP, at only 3.12 kg m^{-3} during the second growing season. The highest net farm income (NFI) was reported for the T-tape GR at 8296.74 US$ y^{-1} (dollars per year), followed by the Bubbler and online PC dripper systems, which yielded net farm incomes of 7568.98 US$ y^{-1} and 7437.07 US$ y^{-1}", respectively. The RZWS had the lowest NFI, amounting to 4408.40 US$ y^{-1}.

Keywords: Microirrigation systems, Saline irrigation water, Remote sensing, Soil moisture distribution patterns, Salt distribution patterns.

1. Introduction

Irrigated agriculture remains largest sector of water consumption in the world, However, the potential for future profitability of large-scale irrigated agriculture is threatened by new water scarcity conditions that include high population pressure densities, global climatic changes, and competition with other sectors of the economy (Saad et al., 2025). Increasing scarcity of water has become one of the most serious limitations to economic growth in arid and semi-arid areas including Egypt, of whose agricultural sector stands as the biggest user of freshwater resources. Due to rising water stress, a number of countries have ended up using non-renewable fossil groundwater to fulfill short term water need. Such a strategy however presents l poling term threats to the performance of the water supply, food security and consequent economic competence. Due to the scarcity of opportunities to increase water supply and the growing pressure on the existing resources, an increase in water productivity is becoming a strategic necessity. In farming we can say that this objective is reflected in the strategy of achieving more crop and high value per drop (Pibars et al., 2025).

In Egypt, which is marked by an arid climate and limited rainfall during the crop growing season, irrigation becomes crucial for achieving optimal agricultural yields. However, the increasing scarcity of water as a natural resource, with agriculture consuming approximately 85% of available water, necessitates that farmers adopt effective irrigation scheduling and water conservation practices. The prevalent inefficiency in water resource utilization in Egypt can be attributed to either suboptimal irrigation efficiency or inadequate scheduling, resulting in the loss of precious water resources, heightened production costs, and adverse

*Corresponding author email: mohamed.aboarab@agr.cu.edu.eg; 11622022421215@pg.cu.edu.eg
Received: 28/08/2025; Accepted: 05/10/2025
DOI: 10.21608/AGRO.2025.418289.1829

environmental consequences (Ouda, 2020a). Water is essential for the growth and development of plants. Without water, the plant endures drought conditions, significantly affecting its growth and ultimately diminishing crop yield. Yield efficiency denotes the productivity of a plant grown in an optimal environment, characterized by adequate availability to water and nutrients, alongside effective management of pests and disease (Mansour, 2025).

Effective water management at the agricultural level is crucial, particularly in the context of establishing suitable irrigation schedules that maximize production while simultaneously optimizing water usage, especially in relation to non-beneficial applications (Ferreira et al., 2023).

While flood irrigation is often viewed as a cost-effective and straightforward method for irrigating orchards, it is associated with significant water loss, nutrient leaching from the root zone, and the spread of soil-borne fungal diseases (Dubey et al., 2019). Traditional irrigation methods, including overhead sprinklers and flooding systems, tend to keep the soil, foliage, and tree trunks moist for extended periods, which can increase the risk of mold and fungal infections. In contrast, flood irrigation not only wastes water but also lacks efficiency compared to drip irrigation, which delivers a precise amount of water directly to the plant's root zone (Olamide et al., 2022). Modern pressurized irrigation systems, such as drip and sprinkler systems, allow for the application of a controlled volume of water to orchards. In addition to conserving water, the drip irrigation system has been shown to enhance the yield of citrus fruits (Al-agele, 2020). This system provides water frequently, often on a daily basis, to sustain optimal soil moisture levels, mitigate moisture stress in plants, and ensure the efficient utilization of water resources (Francob et al., 2025). According to (Dinar, 2024), the enhancement of water productivity (WP) is contingent upon the productivity improvements characterized by a steady increase in output per unit of input, as well as the irrigation methods employed. The advancement of WP in agricultural practices is vital for conserving water resources and achieving greater yields. Contemporary irrigation technologies, including sprinkler and micro irrigation systems, are recognized for their efficiency and significant potential to enhance crop yields. Notably, among the various pressurized irrigation systems, the drip irrigation method is particularly effective in conserving irrigation water compared to both full cover and strip cover sprinkler systems (Chikankheni, 2023).

Soil salinity can develop in diverse climatic conditions, occurring either naturally (primary salinization) or as a result of anthropogenic activities (secondary salinization). This phenomenon is particularly prevalent in arid and semi-arid regions where insufficient rainfall fails to leach salts from the plant root zone, regardless of whether the plants are irrigated or depend solely on precipitation. The primary determinants of soil salinity include geological characteristics, chemical composition, climatic conditions, and local hydrological systems (Salcedo et al., 2022). In agricultural settings, the distribution of salts is neither consistent with soil depth nor stable over time, as it is influenced by irrigation practices and leaching techniques aimed at managing salt concentrations in the root zone, in addition to variations in rainfall (Minhas et al., 2020). Daba and Qureshi (2021) defines soil salinization as the accumulation of salts at the soil surface or within the root zone, which adversely impacts both plant health and soil quality. This accumulation leads to a decline in soil productivity, posing a significant threat to agricultural sustainability. If current trends persist, numerous countries may face challenges in producing adequate food supplies for their populations (Gorji et al., 2017). Soil decay resulting from salinity and sodicity is a main environmental menace to soil fecundity and crop productivity in arid and semiarid areas of the world. The increase of salinity in soil and groundwater is a major concern in Egyptian agriculture because of inadequate drainage conditions and the reduction in Nile demineralization of the soil owing to the deficiency of flooding. About 33% of total land area cropped is salt-affected land in Egypt, characterized as saline-sodic soils due to their poor physical and chemical properties (Ibrahim, 2022). Salt stress affects 20% of global cultivable land and is increasing continuously owing to the change in climate and anthropogenic activities (Elkot et al., 2023). Consequently, the monitoring and forecasting of soil salinity levels are essential for the implementation of strategies aimed at preventing soil degradation (Stavi et al., 2021).

Remote sensing data serve as a valuable resource for calculating various vegetation indices through both straightforward and complex band ratio combinations. Satellite imagery provides an extensive dataset that can be analyzed, processed, and stored to enhance the understanding of different vegetation indices, which are influenced by the specific satellite sensor employed (Zeng et al., 2022). The fundamental objective of employing vegetation indices is to refine the interpretation of spectral data reflected from vegetative cover. Variations in spectral reflectance are instrumental in distinguishing diverse vegetation traits, which are influenced by crop-water interactions and the characteristics of surrounding soil and atmospheric components, thereby optimizing the representation of vegetation features in relation to their

environment (Yan et al., 2025). Key soil attributes such as color, texture, and moisture content significantly impact soil spectral reflectance (Elhag and Bahrawi, 2017). Spectral vegetation indices are derived from mathematical combinations of various spectral bands, primarily within the visible and near-infrared segments of the electromagnetic spectrum. Comprehensive assessments of vegetation activity can be achieved through semi-analytical approaches utilizing spectral band ratios, which have been widely applied to monitor not only the seasonal fluctuations of vegetation cover but also the spatial variability at a local scale (Tshazi, 2022). By integrating data from visible, near-infrared (NIR), and shortwave infrared (SWIR) bands, remote sensing techniques can compute critical vegetation indices, including the Normalized Difference Vegetation Index (NDVI), Soil Adjusted Vegetation Index (SAVI), Modified Soil Adjusted Vegetation Index (MSAVI), and Salinity Index (SI). These indices provide essential insights into plant health, vegetation density, soil salinity, and moisture content (Sishodia et al., 2020, Jindo et al., 2021, Vélez et al., 2023).

Citrus fruits represent a significant agricultural commodity in Egypt and globally, holding the top position in both cultivated area and production within the country (Abd-Elgawad, 2021). The total area dedicated to citrus cultivation is approximately 518,920.84 acres, with a harvested area of 308,202.18 acres, resulting in an export volume of 1,871,150 tons (Alshallash et al., 2022). Renowned for their exceptional taste, flavor, and high vitamin C content, citrus fruits are regarded as the most promising export fruits and are widely favored in Egypt (Khan et al., 2020). Their substantial nutritional value, particularly in vitamin C, contributes significantly to human health by enhancing resistance to influenza and reducing calcium oxalate buildup in the kidneys (Alshallash et al., 2022). Among the various citrus species, the Valencia orange (Citrus sinensis L. (Osbeck)) stands out as the most exported variety in Egypt (Chetto et al., 2025), with its products primarily consumed as juice and enjoying global demand (Alshallash et al., 2022). The late cultivar of Valencia orange is predominantly cultivated in newly reclaimed desert lands under Egyptian conditions (Mansey et al., 2021).

This study aims to achieve several objectives: firstly, to enhance the sustainable management of irrigation water for orange trees grown in sandy soils affected by salinity in both soil and irrigation water, thereby improving ecosystem utilization and increasing farmers' income; secondly, to conduct a comparative analysis of various micro-irrigation techniques to identify the most effective systems for managing soil moisture and salinity levels, ultimately optimizing the yield of orange orchards; and thirdly, to utilize remote sensing indices for the continuous monitoring of plant health and soil salinity throughout the growing season, offering a low-labor approach to assess the effectiveness of water management practices.

2. Materials and Methods

2.1. Study Area

Field experiments were carried out over two consecutive growing seasons, specifically from 2023 to 2024 and from 2024 to 2025, at a citrus orchard that was five years old, organized in a 4 × 5 meter planting configuration. This research was conducted in Regwa, located in the EL-Beheira Governorate of Egypt, with geographical coordinates of approximately 30° 10' 13" N latitude and 30° 44' 49" E longitude, at an elevation of 72.81 meters above sea level (Fig. 1).

The mechanical properties of the soil were evaluated using the pipette method as described by (Dewis and Freitas, 1970). The field capacity (Θ_{fc}) and the permanent wilting point (Θ_{pwp}) were determined through the pressure membrane technique, with measurements taken at 0.33 and 15 Atm, respectively, following the procedures established by Klute and Dirksen (1986). Soil pH was assessed in a 1:2.5 (Soil: Water) suspension according to methodology (Isdory et al., 2021) (Table 1). The bulk density of the soil was calculated using cylindrical samples with sharp edges, which were carefully inserted into the soil to a specified depth to obtain a known volume of undisturbed soil. These samples were subsequently dried in an oven at 105 °C, allowing for the calculation of bulk density in g cm^{-3} as per (Al-Shammary et al., 2018) guidelines (Table 1).

The total water-soluble salts were measured using an electrical conductivity meter on extracts from soil paste, as outlined by Richards (1954). Additionally, the quantification of soluble ions, including Na^{+}, K^{+}, Ca^{+2}, Mg^{+2}, HCO_{-3}, CO_{-3}, SO_{-4}, and Cl^{-}, was conducted in accordance with (Isdory et al., 2021) (Table 2). The irrigation water utilized in the experiments was sourced from a deep well situated at the experimental site, which had a pH of 7.64 and an average electrical conductivity of 7.01 dS m^{-1} (Table 3).

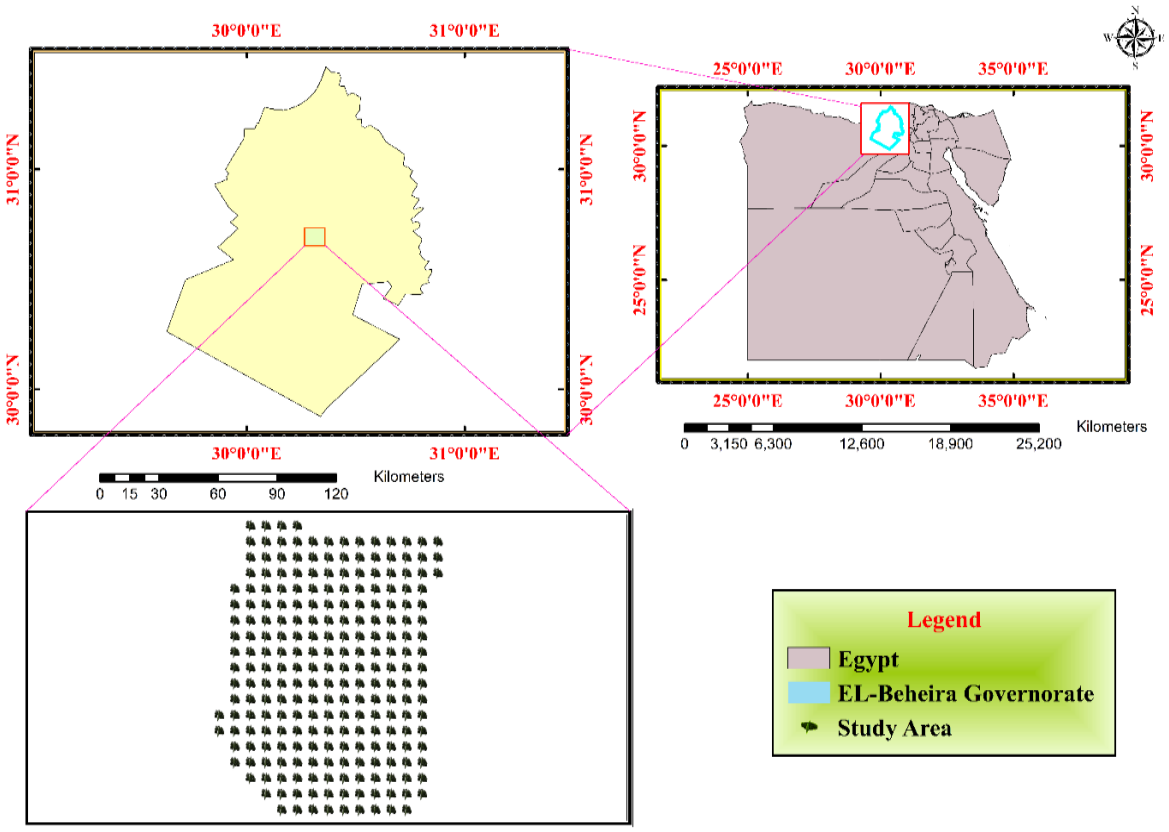

Fig. 1. The Study Area (Source: Digitized from google earth imagery).

Table 1. Physical analyses of the Soil Sample.

Soil Depth (cm)	Soil Particles Distribution				Texture	Θ_{fc}	Θ_{pwp}	ρ	SP (%)
	CS	FS	Silt	Clay		(cm^3 cm^{-3})		(g cm^{-3})	
0 – 10	63.95	10.25	17.7	8.1	Sandy Loam	19.52	8.97	1.63	24.15
10 – 40	57.75	10.25	22.4	9.7	Sandy Loam	18.95	9.21	1.64	20.15
40 – 70	48.05	17.5	23.15	11.3	Sandy Loam	19.05	8.39	1.62	22.40
70 – 100	53.95	8.9	22.55	14.6	Sandy Loam	18.70	8.28	1.61	22.25

SP: Soil permeability, CS: Coarse sand, FS: Fine sand.

Table 2. Chemical analyses of the soil samples.

Soil Depth (cm)	pH	EC_e (dS m^{-1})	TDS (ppm)	Cations (meq L^{-1})				Anions (meq L^{-1})				$CaCO^3$ (%)
				Ca^{+2}	Mg^{+2}	Na^{+}	K^{+}	CO^{-3}	HCO^{-3}	SO_4^{-}	CL^{-}	
0 – 10	8.30	2.85	1824	4.10	4.35	18.6	1.45	ND	5.05	2.80	20.60	1.48
10 – 40	8.59	1.20	768	1.75	1.85	7.8	0.6	ND	2.15	1.20	8.70	1.05
40 – 70	8.70	1.15	736	1.65	1.75	7.5	0.6	ND	2.05	1.15	8.30	1.70
70 – 100	8.76	1.30	832	1.85	2.00	8.5	0.65	ND	2.30	1.30	9.40	2.95

Table 3. Irrigation water chemical analysis.

pH	EC (ds m^{-1})	TDS (ppm)	Cations (meq L^{-1})				Anions (meq L^{-1})		SAR (%)
			Ca^{+2}	Mg^{+2}	Na^{+}	K^{+}	HCO_3	Cl^{-}	
7.64	7.01	4486	18.14	17.98	49.73	.036	4.22	51.60	11.70

2.2. Weather conditions

The experimental site is defined by its arid climate, which is marked by frigid winters and intensely hot, dry summers. Throughout the growing seasons of 2023-2024 and 2024-2025, meticulous daily weather data were gathered from freely accessible data sourced from the NASA website, with a high-resolution daily time series of 0.5 * 0.5 degrees (Okal et al., 2020, Mompremier et al., 2021). This dataset encompassed maximum temperature (T_{max}), minimum temperature (T_{min}), relative humidity (RH), wind speed (WS), solar radiation (Rn), and precipitation (Pe), culminating in a comprehensive dataset for further analysis as presented in (Table 4).

Table 4. Monthly environmental condition variables as an average for the two cultivated seasons.

Year	Month	T_{min} (°C)	T_{max} (°C)	RH (%)	WS (m s^{-1})	Rn (W m^{-2})	Pe (mm)
2023-2024	February	6.35	18.98	67.65	2.54	92.32	0.37
	March	6.60	20.25	62.10	2.95	115.27	1.29
	April	12.54	30.43	49.65	3.22	133.78	0.0
	May	15.96	32.92	44.92	3.34	149.02	0.0
	June	20.49	37.05	45.08	3.42	154.78	0.0
	July	20.63	37.85	46.77	3.36	153.89	0.10
	August	22.03	37.82	48.86	3.11	140.58	0.04
	September	20.86	36.14	50.91	3.07	122.89	0.06
	October	17.06	29.58	59.09	2.86	98.79	0.11
	November	13.01	24.79	60.77	2.21	85.73	0.01
	December	11.21	22.66	64.88	2.28	85.73	0.54
	January	7.98	20.38	63.88	2.14	73.98	0.12
2024-2025	February	6.55	19.36	62.67	2.43	92.32	0.08
	March	10.80	25.35	50.26	2.89	115.27	0.17
	April	12.98	29.13	48.30	4.78	139.19	0.0
	May	16.79	33.21	45.21	5.55	155.04	0.0
	June	20.46	36.65	43.80	5.75	161.03	0.0
	July	22.22	40.00	44.50	5.58	160.11	0.10
	August	22.54	38.89	48.25	5.33	146.26	0.04
	September	21.87	37.28	47.45	4.75	127.86	0.06
	October	18.75	31.79	59.81	4.33	102.78	0.11
	November	14.72	26.65	61.08	3.77	89.19	0.01
	December	11.21	22.42	67.31	3.85	89.19	0.54
	January	7.71	19.89	57.68	4.01	77.41	0.11

2.3. Crop evapotranspiration and irrigation scheduling

The assessment of crop evapotranspiration was conducted in accordance with the protocols established by the Food and Agriculture Organization of the United Nations (FAO). The reference evapotranspiration (ET_o) was determined utilizing the Modified Penman-Monteith equation as detailed in FAO 56 (Djaman et al., 2018), incorporating daily meteorological data gathered from the experimental site. The calculations for ETo were supported by the FAO's online calculator (http://www.fao.org/land-water/databases-and-software/eto-calculator/en/) and supplemented with additional software tools such as CLIMWAT 2.0 and CROPWAT 8.0, which were employed to estimate the evapotranspiration specific to orange cultivation, following the methodologies presented in Equation 1.

$$ET_o = \frac{0.408\Delta(R_n - G) + \gamma \frac{900}{T+273} U_2 (e_s - e_a)}{\Delta + \gamma(1 + 0.34U_2)} \quad (1)$$

In this context, ET_o is defined as the reference evapotranspiration measured in millimeters per day (mm d^{-1}), with R_n representing the net radiation received at the crop surface (MJ m^{-2} d^{-1}). The soil heat flux density is denoted by G (MJ m^{-2} d^{-1}), T indicates the average daily air temperature at a height of 2 meters (°C), and U_2 refers to the wind speed at the same height (m s^{-1}). Furthermore, e_s and e_a represent the saturated and actual vapor pressure deficits, respectively (kPa). The methodology for estimating the crop's evapotranspiration is grounded in the principles and techniques outlined in FAO Irrigation and Drainage Paper No. 56 (Djaman et al., 2018), which elucidates the daily water requirements of the plant through the interplay of soil evaporation and leaf transpiration, following the methodologies presented in Equation 2.

$$ET_C = ET_O \times Kc \quad (2)$$

where K_c represents the crop coefficient, ET_O represents the daily reference evapotranspiration (mm day^{-1}), and ET_C represents the crop's evapotranspiration.

Irrigation efficiency, represented as E_i, is quantified as a percentage, while R signifies the volume of water accessible to the plant from non-irrigation sources, measured in millimeters (mm). LR, on the other hand, denotes the volume of water required for the effective leaching of salts, also expressed in millimeters (mm), J LR, on the other hand, denotes `WERthe volume of water required for the effective leaching of salts, also expressed in millimeters (mm), highlighting the intricate dynamics of irrigation management in agricultural systems. The crop coefficient, referred to as K_c, is crucial for assessing irrigation needs, while ET_o indicates the daily reference evapotranspiration, measured in millimeters per day. The gross irrigation requirements for orange trees are calculated following the framework proposed by (Ouda, 2020b), which provides a systematic method for determining the water essential for optimal crop growth, The gross irrigation requirements for orange were calculated by the following equation (3).

$$IR_g = \left(\frac{ET_O \times K_C \times K_r}{E_i}\right) - (R + LR) \quad (3)$$

In this framework, IR_g represents the gross irrigation requirements in millimeters per day, with ET_o again denoting the reference evapotranspiration in the same unit. The crop coefficient K_c is sourced from (Salemi et al., 2020), while K_r indicates the ground cover reduction factor. The specific values for Kr should be determined using Keller's equation (4), as outlined by Sefrin et al. (2020), which contributes to a deeper understanding of the elements influencing irrigation efficiency. Furthermore, GC is defined as the percentage of ground cover, calculated by comparing the shaded area of each plant to the total area it occupies.

$$K_r = GC + 0.15(1 - GC) \quad (4)$$

Where, the ground cover percentage (GC) is defined as the ratio of the shaded area produced by individual plants to the total area they occupy.

2.4. Crop administration

The research specifically examined the 'Valencia' cultivar of orange (Citrus sinensis), recognized for its late maturation and superior fruit quality. A significant challenge faced by Valencia oranges is their propensity to yield smaller fruit sizes, which, along with the occurrence of fruit creasing, adversely affects their marketability, as larger fruits tend to fetch higher prices in the export market (Mossad et al., 2020). Consumer preferences favor larger fruits, leading to a considerable price gap between large and small oranges (Napitupulu et al., 2025).

2.5. System installation and experimental treatments

Field investigations involve the examination of six distinct irrigation methods: T-tape GR drippers, the Root Zone Watering System (RZWS), online drippers, online PC drippers, mist sprayers, and bubblers (Fig. 2). Notably, The RZWS, engineered by Hunter Industries, is tailored to deliver water directly to the active root zone of the orange tree with optimal efficiency. This system comprises perforated tubing, a water flow regulator, and a surrounding gravel layer. The tubing has a diameter of 75 mm and a length of 45 cm, encased in filtering cloth and gravel to prevent fine soil particles and roots from infiltrating the perforated areas. Under steady-state flow conditions, gravitational forces

significantly affect water movement within the soil. The RZWS operates at a discharge rate of 114 L h^{-1} and a pressure of 2 bar, positioned 50 cm from the orange tree. In the drip irrigation configuration, each orange tree is outfitted with four drippers of three distinct types. The lateral line, constructed from polyethylene with a diameter of 16 mm, features a 100 cm spacing for the Katif PC online dripper (Rivulis), which operates at 8 L h^{-1} and 1 bar operating pressure. The second type, the J-Turbo Key plus (Jain Irrigation Systems), also functions at 8 L h^{-1} and 1 bar pressure. The final type, T-tape GR drippers (Eurodrip, Rivulis), are spaced 50 cm apart and operate at 7.5 L h^{-1} with a pressure of 1 bar. Each Orange tree is also equipped with the Bubbler PCN-50 from Hunter Industries, which provides a flow rate of 114 liters per hour at an operating pressure of 2.0 bar. Furthermore, The Rivulis Rondo Mist Sprayers are assigned to each tree, delivering a flow rate of 47 liters per hour at an operating pressure of 2.5 bar, featuring a black nozzle of 0.85 mm that achieves a wetting diameter of 2 meters. Both the bubbler and mist sprayer are connected to the lateral line through flexible micro tubing with a diameter of 5 mm.

The irrigation system was equipped with an electric submersible pump that had the capacity to discharge 100 cubic meters per hour, functioning at a pressure head of 10 bar, and driven by a 58.8 kW electric motor. The control head comprised critical components including a shut-off valve, safety valve, non-return valve, fertilizer injection pump, screen filter, flow meter, pressure gauges, and an air vent valve. The mainline was constructed using a 160 mm PVC pipe to effectively transport and distribute irrigation water from the well to the sub-mainline. A specialized valve and a highly precise flow meter, with an accuracy of 0.0001 m^3, were integrated to manage the water supply. The sub-main line was fabricated from 90 mm PVC pipe, specifically designed for the efficient conveyance and distribution of water from the main line to the sub-line. The manifold line utilized 63 mm PVC piping, which is essential for the distribution of irrigation water from the manifold to the lateral lines. Lastly, polyethylene lateral lines with a diameter of 16 mm were utilized to carry and distribute irrigation water from the manifold to various irrigation systems.

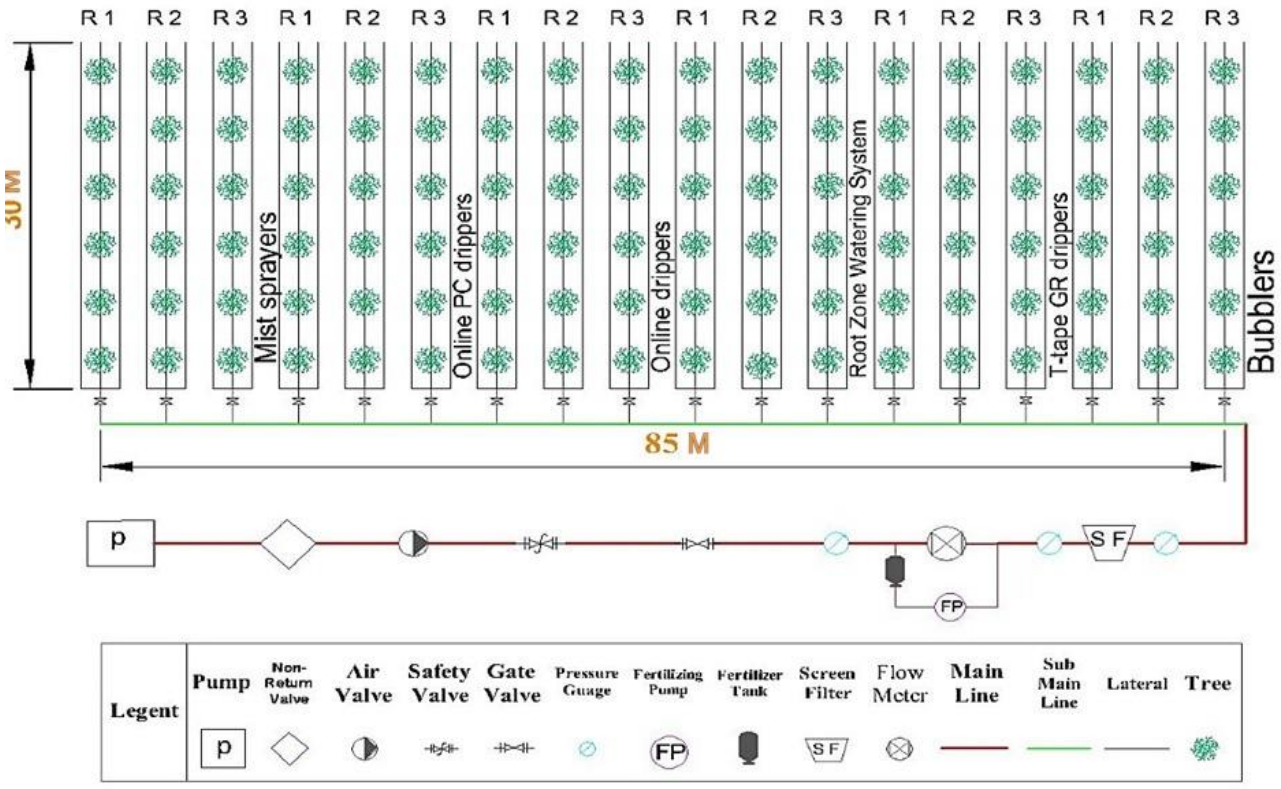

Fig. 2. A hydraulic diagram of the micro-irrigation system and treatments.

2.6. Field Measurements

2.6.1. Irrigation systems evaluation

The assessment of hydraulic properties was conducted at the orange farm, affiliated with the Higher Institute of Agricultural Cooperation in Regwa, situated in the EL-Beheira Governorate of Egypt. To evaluate the consistency of water application, the statistical distribution of dripper flow rates was scrutinized, employing the coefficient of variation (ν) and emission uniformity (EU) as delineated by equations (5) and (6) (Karmeli and Keller, 1975).

$$\nu = \frac{sd}{q_a} \quad (5)$$

$$EU = 100\left(1.0 - 1.27\frac{\nu}{\sqrt{N'_p}}\right)\frac{q_n}{q_a} \quad (6)$$

Where, sd denotes the standard deviation of dripper discharge (L h^{-1}), q_a represents the mean dripper flow rate (L h^{-1}), ν is the coefficient of variation provided by the manufacturer, N'_P indicates the number of emitters per plant, q_n refers to the minimum discharge rate (L h^{-1}). The evaluation of subsurface drip irrigation (SDI) systems was categorized into five levels of micro-irrigation uniformity, ranging from excellent to unacceptable, as defined by the American Society of Agricultural Engineers (Lamm et al., 2021) (Table 5).

Table 5. Hydraulic characteristic of the trickle irrigation system.

Characteristics	Emitter type		
	T-tape (GR)	Online PC	Online
Wall Thickness (mm)	1.15	1.20	1.20
Internal diameter (mm)	13.7	13.6	13.6
Pressure compensating	No	No	No
Minimum operating pressure (bar)	0.29	0.29	0.29
Maximum operating pressure (bar)	1.0	1.0	1.0
Emitter flowrate (L h-1)	7.5	8.4	8.0
Emitter spacing (cm)	50	100	100
Lateral spacing (cm)	100	100	100
Exponent (x)	0.49	0.00	0.48
C_V	0.09	0.04	0.09
EU	92.77	83.96	81.59

Furthermore, to ascertain the optimal configuration for water distribution on the soil surface utilizing mist sprayer irrigation system, the application uniformity was assessed to determine the reliability of water distribution across varying discharge rates, operational pressures, and nozzle heights. The Christiansen uniformity coefficient (CU) and distribution uniformity (DU) were utilized to compute application uniformity, with the Christiansen uniformity coefficient, a recognized benchmark for evaluating application uniformity, being introduced by Christiansen (1942) and calculated accordingly, The Christiansen uniformity coefficient (CU) were calculated by the following equation (7).

$$CU = 100(1.0 - \frac{\sum_{i=1}^{n}|z-m|}{\sum_{i=1}^{n} z}) \quad (7)$$

Where, the Christiansen uniformity coefficient (CU) serves as a critical metric, where z denotes the individual depths of catch measurements obtained during the uniformity assessment (measured in millimeters), m represents the mean depth of these measurements, and n indicates the total number of observations, as articulated by Keller and Bliesner (1990). The concept of distribution uniformity is expressed as a percentage, reflecting the ratio of the average low-quarter volume of water-whether captured or infiltrated to the average total volume captured or infiltrated, as outlined in the equation (8) proposed by James (1988).

$$DU = 100\frac{\overline{X}_{LO}}{\overline{X}} \quad (8)$$

Where, $\overline{X}_{LO}$ is the average low-quarter volume (mm) and $\overline{X}$ is the average total volume (mm) are pivotal indicators of the overall water

captured or infiltrated. The Christiansen uniformity coefficient, in conjunction with distribution uniformity, is relevant across a range of micro-irrigation systems, such as mist sprayers, root zone watering systems (RZWS), and bubblers, as demonstrated in (Table 6).

Table 6. Hydraulic characteristic of the microirrigation systems.

Evaluation parameter	Mist sprayer	RZWS	Bubbler
CU	90.72	97.94	81.32
DU	88.54	97.00	83.59

2.6.2. Soil moisture and salt distribution in root zone

The evaluation of soil moisture levels and salt distribution was conducted under various micro-irrigation systems at five specified distances from the orange tree, namely 0, 50, 100, 150, and 200 cm along the X-axis (soil surface), and at five distinct depths from the surface, specifically 0, 10, 40, 70, and 100 cm along the Y-axis. This analysis was performed two hours after irrigation. To accurately measure soil water content, the weight method was utilized, which enabled precise calculations of irrigation needs and the monitoring of soil moisture conditions critical for crop development during essential growth stages such as planting, flowering, and fruit maturation.

Soil samples were obtained using an auger at the predetermined depths, subsequently placed in airtight zipper bags, and labelled with their corresponding locations, coordinates, dates, and unique identification numbers. Prior to analysis, the samples underwent a dehydration process, which involved placing 50 g of fresh soil in a container on a scale to record the moisture content along with the date, time, depth, and sample number. The samples were then subjected to oven drying at 105 °C for a duration of 24 hours until a stable weight was reached. Following the drying process, the containers were weighed to ascertain the dry weight of the soil, and the soil moisture content was calculated using the formula (9) proposed by Batjes et al. (2020).

$$\text{Soil moisture content (\%)} = \frac{\text{Weight of the moist soil (g)} - \text{Weight of the dry soil (g)}}{\text{Weight of the dry soil (g)}} \times 100 \quad (9)$$

In order to depict the distribution of soil moisture and salinity through contour lines and to investigate the fluctuations of these parameters within the soil profile, the Surfer software was employed. This software excels in converting three-dimensional data into visual cartographic formats. The data were input into the model utilizing X, Y, and Z coordinates, where X denoted the positions of access tubes or sites (S1, S2, and S3) in relation to the emitter, sprayer, bubbler, and RWS. Y represented the recorded soil depths (0, 10, 40, 70, 100 cm), while Z indicated the levels of soil moisture and salinity. Furthermore, The Surfer model was utilized to assess the dynamics of soil water and salt movement throughout the soil profile.

2.6.3. Flowering and fruiting behavior

The time required for the formation of flower buds was evaluated by observing a randomly selected sample of 60 buds, sourced from 4 branches of 15 different plants (with one bud per branch). These buds were marked immediately upon their appearance, and their development was meticulously monitored from the beginning of the flowering shoot until the flowers were fully open.

2.6.3.1. Fruit set percentage

Data regarding fruit set were collected following complete blooming, with the percentage of fruit set calculated based on the ratio of flowers to the number of fruits that successfully developed. The calculation of fruit set percentage was performed using the formula (10) established by (Alcaraz and Hormaza, 2021).

$$Fruit\ set\ \% = \frac{Total\ number\ of\ fruit\ set}{Total\ number\ of\ flower} \times 100 \quad (10)$$

2.6.3.2. Percentage of fruit drop

To assess fruit drop, the total number of fruits remaining on the branch at harvest was subtracted from the initial count of fruits that had set on the branch. The percentage of fruit drop was then calculated using the method described by Kumar et al. (2018), The Percentage of fruit drop were calculated by the following equation (11).

$$Fruit\ drop\ (\%) = \frac{Total\ number\ of\ fruit\ drop}{Total\ number\ of\ fruit\ set} \times 100 \quad (11)$$

2.6.4. Production and fruit properties

2.6.4.1.Total yield and productivity

The yield was evaluated at the time of maturity during the final week of January each year. All

fruits from every tree were gathered and weighed to compute the average yield per tree in kilograms. To analyze the effects of various irrigation systems on yield, each tree subjected to different treatments in the experiment was harvested separately, and the oranges from each tree were weighed to ascertain the yield per tree in kilograms (Mengü et al., 2024).

2.6.4.2. Physical fruit properties

At the point of fruit maturity, samples of oranges were randomly collected from the southern aspect of trees and various orchards, as noted by (Domingues et al., 2020), following the growing season in January. For each replicate tree, ten Valencia oranges were selected, resulting in a total of 30 fruits per treatment, to determine the average fruit weight (g per fruit) using an electronic balance with a precision of 0.01 g. The principal diameters of the fruits were measured with an accuracy of 0.01 mm across three main axes, while the pulp diameter and rind thickness were assessed using a digital Vernier caliper at the maturity stage. The actual volume of each fruit was determined by employing a graduated beaker with a one-liter capacity. The beaker was filled with water to a specific level, and the fruit was fully submerged using a glass rod. The actual volume of the fruit (V) was then calculated by finding the difference between the two recorded water volumes for each individual fruit, The actual volume of the fruit (V) were calculated by the following equation (12).

$$\text{Volume } (\text{cm}^3) = \frac{\text{displaced water (g)}}{\text{water density (g cm}^{-3})} \quad (12)$$

To extract juice from the fruits, a rotary squeezer was utilized, and the resulting juice was filtered through a sieve with a mesh size of 0.8 mm. The weight of the extracted juice was measured using an electronic balance, and the percentage of juice was calculated by following the equation (13) outlined by (Nnamdi et al., 2020).

$$\text{Juice } (\%) = \frac{\text{Juice weight (g)}}{\text{Fruit weight (g)}} * 100 \quad (13)$$

The rag percentage was determined using the following formula (14):

$$\text{Rag } (\%) = \text{Fruit weight} - \frac{\text{Juice weight + Peel weight}}{\text{Fruit weight}} * 100 \quad (14)$$

The mean geometrical diameter (GM) was determined using the following formula (15):

$$\text{GM} = (\text{ac}^2)^{\frac{1}{3}} \quad (15)$$

Where, GM represents the mean geometrical diameter measured in millimeters (mm), while 'a' denotes the primary longest diameter also in millimeters (mm), and 'c' signifies the longest diameter that is perpendicular to both 'a' and 'b', measured in millimeters (mm). The surface area (S) was determined using the following formula (16):

$$S = \pi \text{GM}^2 \quad (16)$$

The aspect ratio (Ra) was determined using the following formula (17):

$$R_a = \left(\frac{c}{a}\right) * 100 \quad (17)$$

The rind ratio (Rs) was determined using the following formula (18):

$$R_s = \frac{M_s}{M_f} * 100 \quad (18)$$

Where, the aspect ratio (Ra) is defined as a percentage, while the rind ratio (Rs) is also expressed as a percentage. The rind mass (Ms) is measured in grams, and the fruit mass (Mf) is similarly quantified in grams. The leaves were meticulously detached, washed with tap water, and weighed using a digital electronic balance. Following this, the leaves were dried in an oven set to 80°C for a duration of 48 hours to determine their dry weight. Mature, fully expanded, and uniform leaves from the Th_1, Th_2, and Th_3 plants were selected to assess leaf water loss (WL) during the period from 10:30 am to 11:30 am. Any moisture on the leaf surfaces was carefully blotted with filter paper, and the fresh weight (FW_0) was recorded immediately. The leaves were then positioned with their abaxial side facing upwards on a clean surface to allow for transpiration, under controlled conditions of room temperature ranging from 25 to 28 °C and an air relative humidity of 65%. Each leaf's weight was measured at 30-minute intervals (FW_t) over a 24-hour period. Ultimately, all leaves were subjected to oven drying at 70 °C for 48 hours and re-weighed to ascertain their dry weight (DW). The measurements of FW_0, FW_t, and DW were subsequently employed to calculate the leaf water loss (WL) using a designated equation (19) (Gunny et al., 2024).

$$\text{WL} = \frac{(FW_0 - DW) - (FM_t - DW)}{(FW_0 - DW)} \text{ x } 100 \quad (19)$$

Furthermore, four leaves were randomly selected from each treatment across all replications, and their areas were quantified using the graph paper method to establish the single leaf area in square centimeters. The average leaf area for each leaf was then computed and recorded. Additionally, the chlorophyll content, represented in SPAD units, was evaluated in the fresh leaf samples using a Minolta SPAD chlorophyll meter (Martínez et al., 2017).

2.6.4.3. Mechanical fruit properties

Fruit firmness (FF lb in^{-2}) was assessed in both the peel and pulp of the fruit using a pressure tester, specifically the Digital Force-Gouge

Model FGV-0.5A to FGV-100A from Shimpo Instruments, as noted by Ibrahim and Gad (2015). The required penetration force and firmness were evaluated with a penetrometer equipped with various head tools. The 6.4 mm diameter head tool was utilized for measuring the penetration force, while the 15 mm diameter head tool was employed to assess firmness. Measurements of the penetration force were conducted along both the longitudinal and horizontal axes of each fruit.

2.6.4.4. Chemical fruit properties

pH levels were determined using a digital pH meter (Nig 333, Naina Solaris LTD, India) after homogenizing 10 ml of fruit juice with 90 ml of distilled water, as described by (Erkmen and Bozkurt, 2004). Total sugar content was estimated following the methodology outlined by (Tiencheu et al., 2021). The standard procedure for measuring titratable acidity was applied, as referenced (Kasapidou et al., 2025). A 5 mL sample of fruit juice was homogenized in 20 mL of distilled water and subsequently filtered through Whatman No.1 filter paper. To the 20 mL of filtrate, two to three drops of phenolphthalein were added as an indicator, and titration was performed against 0.05M NaOH to ascertain the endpoint of phenolphthalein. The titratable acidity was expressed as grams of lactic acid per 100 grams of juice and calculated using the appropriate formula (20).

$$\mathrm{TA} = \frac{\mathrm{MNaOH\ x\ NaOH\ x\ 0.09\ x\ 100}}{\mathrm{juice\ sample}} * 100 \qquad (20)$$

where TA represents titratable acidity, MNaOH denotes the molarity of NaOH employed (mL), NaOH indicates the quantity of NaOH utilized (mL), and 0.09 signifies the equivalent weight of lactic acid. Total polyphenols were extracted and quantified following a procedure outlined by (Alonso-Vázquez, et al., 2025), where in orange juice (1 mL) was subjected to extraction with 9 mL of 80% methanol for a duration of 30 minutes at ambient temperature. Subsequent to centrifugation at 5000 rpm for 10 minutes, the supernatant was collected for the assessment of total phenolics utilizing the Folin–Ciocalteu method as formulated by (Alonso-Vázquez et al., 2025) with certain modifications. The obtained extract (1 mL) was incorporated into a 25 mL volumetric flask containing 9 mL of distilled water, and 4 mL of 7.5% (w/v) Na_2CO_3 was combined with 1 mL of the diluted sample, which was permitted to stand for 60 minutes prior to measurement in a dark environment.

Total carotenoid content was assessed by utilizing juice samples of 25 mL, which were blended with 80 mL of an extracting solvent (n-hexane/acetone, 1:1). Following 30 minutes of shaking in a separation funnel, the upper layer was retrieved. An additional 15 mL of n-hexane/acetone (1:1, v/v) was incorporated, and extraction continued until the aqueous phase became devoid of color (Moumouni Koala et al., 2013). The combined extraction was then saponified using 5 mL of a 10% (w/v) potassium hydroxide solution in methanol, carried out in a dark environment for 2 hours. Subsequently, The saponified mixture was moved to a separatory funnel and combined with 20 mL of deionized water to facilitate the separation of the upper hexane layer, which contained the carotenoids. The hexane layer was gathered, rinsed twice with 10 mL of deionized water, dehydrated with anhydrous sodium sulfate, and filtered through a 0.45 µm membrane. The absorbance of the hexanic extract was measured at 450 nm, and the carotenoid concentration was determined from a calibration curve based on β-carotene.

DPPH free radical-scavenging capability was assessed following the methodology described by (Vuong et al., 2014). In summary, 150 mL of the extracted sample was combined with 2800 mL of a methanolic DPPH solution and allowed to rest in a dark environment for one hour. The absorbance was recorded at a wavelength of 517 nm. The results were expressed as mg trolox equivalents (TE) per 100 mL of sample (mg TE 100 mL^{-1}).

For the assessment of total soluble solids percentage, the extraction of juice from the fruit was conducted via a juicer as outlined by (Elhosary et al., 2023). Subsequently, TSS was evaluated (in triplicate) utilizing a Digital refractometer (ATago. PAL-1. Japan) in accordance with the AOAC protocol (McKie and McCleary, 2016). The TSS/acid ratio was calculated by dividing the TSS measurement by the total acidity level following the methodology established by (Ibrahim and Gad, 2015).

The total vitamin C content in orange juice was quantified following the method detailed by (Vuong et al., 2014). A solution was formulated by blending 5.32 g of sodium phosphate with 2.47 g of ammonium molybdate in 500 mL of 0.6 M sulfuric acid. To this, 0.3 mL of the diluted sample was introduced into 3 mL of the prepared solution and incubated in a water bath maintained at 95 °C for 90 minutes. Following incubation, the absorbance of the solution was measured using a UV–Vis spectrophotometer (Varian Australia Pty. Ltd. , Melbourne, VIC, Australia) at 695 nm and was compared to an ascorbic acid standard (spanning 6.25–100 µg mL^{-1}). The findings were expressed as milligrams of ascorbic acid equivalents (AAE) per 100 mL of sample (mg AAE 100 mL^{-1}).

Total soluble sugars (Brix) were assessed following the methodology of (Shamili, 2019)

utilizing a hand refractometer at ambient temperature. The extraction and quantification of soluble sugars (total sugar, glucose, fructose, and sucrose) were conducted as described by (Omokolo Ndoumou et al., 1996). This approach and the resulting extract were employed for the analysis of sugars. The measurements for total sugar, glucose, and fructose content (reducing sugar), along with sucrose (non-reducing sugar), were carried out according to the techniques outlined by (McCready et al., 1950, Ashwell, 1957, Miller, 1959, Handel, 1968), respectively. The content of ascorbic acid (mg 100 mL^{-1} of juice) was evaluated using the indophenol titration technique as per (Shamili, 2019).

2.6.4.5. Macronutrient quantification

The macronutrient composition of orange foliage was methodically examined using desiccated leaf specimens. Fresh leaf materials underwent an intensive drying process inside an air-forced oven, set at a consistent temperature of 70 ºC for a duration of three days to ensure full desiccation. Once dried, the specimens were meticulously ground into a fine powder, which was essential for analyzing the levels of key macronutrients including nitrogen (N), phosphorus (P), potassium (K), calcium (Ca), and sodium (Na). The Kjeldahl technique, with minor adjustments, was utilized to evaluate the total nitrogen level (N), adhering to the methodology proposed by Jackson (1973). Approximately 0. 5 grams of the leaf or fruit sample were mixed with a blend of sulfuric and Perchloric acids. This combination was then heated for ten minutes at a regulated temperature of 50 ºC until a transparent solution was produced, signifying effective digestion. After cooling, the nitrogen content was measured via a steam distillation method, employing 80 mL of 40% sodium hydroxide followed by titration against 0. 1 N sulfuric acid.

The overall concentrations of phosphorus (P) in the dried samples were analyzed following the procedure outlined by Chen et al. (Moursy et al., 2023). In this method, 3 mL of 30% v:v hydrogen peroxide and 5 mL of 98% sulfuric acid were utilized to digest 100 mg of the desiccated powder. The digested mixture was subsequently allowed to cool to room temperature and diluted with deionized water to achieve a final volume of 100 mL. The phosphorus levels in the prepared solution were assessed using the molybdate blue method, and the absorbance was recorded at 700 nm using a spectrophotometer.

The quantification of potassium (K), calcium (Ca), and sodium (Na) concentrations in the dried samples was performed by implementing the methodology described by Junsomboon and Jakmunee (2020). A solution comprising 50 mL of water and 5 mL of hydrochloric acid was used to homogenize 1 g of the ground sample. This homogenate was then heated on a hot plate for fifteen minutes to promote digestion. Following cooling, the digested mixture was filtered through Whatman No. 42 filter paper. Afterward, distilled water was added to the filtrate to adjust it to a final volume of 100 mL using a volumetric flask. The individual component concentrations were subsequently measured utilizing a flame photometer.

Proline was quantified using the procedure outlined by (Sanaa and Abd El-Rahman, 2023). For each leaf sample, 0.2 g of fresh young tips was collected and immersed in liquid nitrogen for 2-3 minutes. Subsequently, the tissues were disrupted using a tissue miser and homogenized with 4 ml of 3% sulfosalicylic acid for five minutes at ambient temperature. The resulting homogenate was centrifuged at a speed of 3000. Following centrifugation, the mixture was filtered through Whatman-2 filter paper, and the supernatant was then combined again with 4 mL of 3% sulfosalicylic acid. The filtrates were subjected to a reaction with 2 cm^3 of acid ninhydrin in a test tube placed in a boiling water bath for one hour. The reaction was subsequently halted by transferring the mixture to an ice bath. After extracting the resultant mixture with 4 cm^3 of toluene, the tubes were allowed to cool to room temperature. The results were expressed on a dry weight basis of mg g^{-1}.

2.6.4.6 Irrigation water productivity (IWP)

Irrigation water productivity (IWP) serves as a crucial metric for evaluating the efficient utilization of irrigation water within agricultural contexts. The determination of IWP adheres to the approach described in earlier research (Moursy et al., 2023). The Irrigation water productivity (IWP) was determined using the following formula (21).

$$IWP = \frac{E_y}{I_r} \quad (21)$$

where IWP represents the irrigation water productivity specific to a given crop (kg m^{-3}). Here, E_y signifies the economic yield quantified in kg ha^{-1}, while I_r refers to the total quantity of irrigation water deployed, denoted in m^3 ha^{-1}.

2.7. Remote sensing calculations and field measurements

The images employed in this research were sourced from the Sentinel-2 satellite, a component of the Copernicus initiative launched by the European Commission and overseen by the European Space Agency (ESA). This satellite was launched into orbit in June 2015 and functions in a sun-synchronous orbit at an

altitude of 786 kilometers, achieving equatorial crossing at 10:30 a. m. at the descending node. The main instrument utilized for terrestrial observation is the multispectral instrument (MSI), which employs a filter-based push broom imaging approach to collect data across thirteen spectral bands in both the visible and near-infrared (VNIR) and shortwave infrared (SWIR) ranges, providing three distinct spatial resolutions. The essential attributes of the MSI spectral bands for the Sentinel-2 satellite are presented in (Table 7).

Table 7. Main characteristics of the multispectral instrument (MSI) spectral bands of Sentinel2 satellite.

Band Number	Central wavelength (nm)	Band width (nm)	Spatial resolution (m)	Description
1	443.9	27	60	Ultra Blue (Coastal and Aerosol)
2	496.6	98	10	Blue
3	560.0	45	10	Green
4	664.5	38	10	Red
5	703.9	19	20	Visible and Near Infrared (VNIR)
6	740.2	18	20	VNIR
7	782.5	28	20	VNIR
8	735.1	145	10	VNIR
8a	764.8	33	20	VNIR
9	945.0	26	60	Short Wave Infrared (SWIR)
10	1373.5	75	60	SWIR
11	1613.7	143	20	SWIR
12	2202.4	242	20	SWIR

The radiometric resolution of the MSI is 12 bits per pixel, which facilitates 4096 grey levels within the pixel digital values. The MSI captures 13 spectral bands, consisting of four bands with a spatial resolution of 10 meters, six bands at a resolution of 20 meters, and three bands at a resolution of 60 meters, while the width of the orbital swath is 290 kilometers. The images analyzed in this study were at Level 2A, as described by Gascon et al. (2017), reflecting the top-of-atmosphere (TOA) normalized reflectance in cartographic geometry for every spectral band. The images were projected utilizing the Universal Transverse Mercator (UTM) system. These images are accessible to the public via ESA through the Copernicus Open Access Hub (https://Scihub.Copernicus.Eu/Dhus/Home).

Monthly images from Sentinel-2a, covering the period from February 2023 to January, were examined to derive seven vegetation indices: BI, IPVI, NDVI, GNDVI, MSAVI, SAVI, and SI. This examination was conducted using ArcGIS version 10. 8 (Table 8). The Sentinel-2a scenes used in this research were acquired without charge from the official Copernicus Open Access Hub, administered by the European Space Agency (ESA) as part of the Copernicus Program (ESA, 2018).

Table 8. Vegetation indices and remote sensing data description.

Index	Platform	Spatial Resolution (m)	Data Level	Year
BI	Sentinel2 MSI + Sensor	10	Level-2A	From February 2023 to January 2025
IPVI	Sentinel2 MSI + Sensor	10	Level-2A	From February 2023 to January 2025
NDVI	Sentinel2 MSI + Sensor	10	Level-2A	From February 2023 to January 2025
GNDVI	Sentinel2 MSI + Sensor	10	Level-2A	From February 2023 to January 2025
SAVI	Sentinel2 MSI + Sensor	10	Level-2A	From February 2023 to January 2025
MSAVI	Sentinel2 MSI + Sensor	10	Level-2A	From February 2023 to January 2025
SI	Sentinel2 MSI + Sensor	10	Level-2A	From February 2023 to January 2025

2.7.1. Multi-temporal image analysis

2.7.1.1. Brightness Index (BI)

BI signifies the mean brightness of a satellite image. The outcome resembles a panchromatic image while maintaining the same resolution as the original. Consequently, this index is responsive to soil brightness, which is closely linked to soil moisture and the existence of salts on the surface. The Brightness Index correlates with the luminosity of soils, which, in turn, is affected by moisture content, salt presence, and the level of organic matter at the soil surface (Escadafal, 1989), The Brightness Index (BI) was determined using the following formula (22).

$$BI = \frac{\sqrt{R^2+G^2}}{2} \quad (22)$$

where G and R are reflectance in green and red bands.

2.7.1.2. Infrared Percentage Vegetation Index (IPVI)

Crippen (1990) discovered that the decline in NDVI was insignificant and proposed this index to enhance the calculation of the vegetation index. The IPVI values range strictly from 0 to 1, in contrast to NDVI. This index is designed to remove negative values found in NDVI. Functionally, IPVI and NDVI are equivalent, The Infrared Percentage Vegetation Index (IPVI) was determined using the following formula (23).

$$IPVI = \frac{NIR}{NIR+RED} \quad (23)$$

2.7.1.3. Normalized Difference Vegetation Index (NDVI)

The NDVI, one of the earliest remote sensing analytical products used to simplify the complexities of multispectral imagery, is now the most popular index used for vegetation assessment (Huang, 2021). It can be mathematically expressed as the following equation (24):

$$NDVI = \frac{NIR-RED}{NIR+RED} \quad (24)$$

Due to the normalization aspect of its computation, NDVI values range from -1 to 1, indicating a high sensitivity to green vegetation, even in regions with limited vegetation cover.

2.7.1.4. Green Normalized Difference Vegetation Index (GNDVI)

GNDVI, which stands for Green Normalized Difference Vegetation Index, represents a modification of the NDVI intended to improve sensitivity to variations in chlorophyll content within agricultural crops. Throughout all data collection intervals and during both experimental stages, the GNDVI index exhibited the most robust correlation with leaf nitrogen content and dry matter. It was shown to be more efficient than NDVI in differentiating various levels of chlorophyll concentration, which are closely associated with nitrogen content, across two plant species (Viña and Gitelson, 2010), The Green Normalized Difference Vegetation Index (GNDVI) was determined using the following formula (25).

$$GNDVI = \frac{NIR-GREEN}{NIR+GREEN} \quad (25)$$

2.7.1.5. Soil-Adjusted Vegetation Index (SAVI)

The SAVI index, introduced by Lillesand and Kiefer (2004), is acknowledged as a dependable and extensively employed method for the assessment of vegetation. This index leverages the distinctive absorption traits observed in the red spectrum, as well as the heightened reflectance seen in the Near-Infrared (NIR) spectrum. A notable aspect of SAVI is its adjustment to a standardized baseline, which produces values that span from -1 to 1, thus allowing for the comparison of SAVI values from different image sources. Developed to mitigate the influence of underlying soil on the Normalized Difference Vegetation Index (NDVI), SAVI effectively reduces the impact of soil moisture on the index. The formulation for calculating SAVI is presented in Equation (26).

$$SAVI = \frac{\lambda_{NIR}-\lambda_{RED}}{(\lambda_{NIR}+\lambda_{RED}+L)} \times (1+L) \quad (26)$$

where L represents a constant. When L is adjusted to zero, SAVI becomes equivalent to NDVI, with numerous studies often suggesting a value of 0.5 for L. Nonetheless, a choice of 0.1 is made to better represent the soil conditions found in southern Idaho.

2.7.1.6. The Modified Soil Adjusted Vegetation Index (MSAVI)

The Modified Soil-Adjusted Vegetation Index (MSAVI) was developed to address the limitations of the traditional Soil-Adjusted Vegetation Index (SAVI), particularly in areas with sparse vegetation cover where the soil background can considerably influence the vegetation signal (Qi et al., 1994). MSAVI enhances the detection of vegetation by incorporating a dynamic soil correction factor that accounts for variations in soil reflectance, The Modified Soil Adjusted Vegetation Index (MSAVI) was determined using the following formula (27).

$$MSAVI = \frac{\left(2\times NIR+1-\sqrt{((2\times NIR+1)^2-8\times(NIR-RED))}\right)}{2} \quad (27)$$

The computation of MSAVI relies on the near-infrared reflectance (NIR), which is strongly reflected by vegetation, and the red reflectance (RED), which is predominantly absorbed by vegetation. The MSAVI equation also considers the variation in soil brightness.

2.7.1.7. Salinity index (SI)

The salinity index is utilized to represent the level of salt concentrations found in soils. Soil salinization is a common type of land degradation, especially prominent in arid and semi-arid areas where rainfall is greater than evaporation. Elhag (2016) provided the formula (28) for mapping soil salinity.

$$SI = \frac{(Green \times RED)}{BLUE} \quad (28)$$

The calculations for the indices were conducted using the "Raster Calculator" feature available within ArcGIS 10.8 (Zieg and Zawada, 2021, Inácio et al., 2023), as indicated in the formulas presented earlier. The resulting raster images were superimposed onto the defined boundaries of the respective fields, which were created with Google Earth Pro software. These overlays were then exported as KML files and subsequently imported into ArcGIS 10.8 to enable statistical evaluation, the "Band Collection Statistic" tool was utilized, allowing for an extensive multivariate analysis of the raster band collection. This analysis involved determining variance in relation to the mean as well as calculating the correlation coefficient, which depicted the relationships between the data sets. In this research, for Sentinel2, the operational biophysical parameter products were processed via the Sentinel Application Platform (SNAP) toolbox, developed using an artificial neural network (ANN) trained on simulated spectra generated from well-established radiative transfer models (RTMs). The European Space Agency (ESA) offers a robust Open Source Radar Software (OSRS) tool specifically intended for Sentinel data. The SNAP Toolbox (ESA 2018) can be accessed and installed on a personal computer from http://step. esa. int/main/download/. It is available in both 32-bit and 64-bit formats.

The indices were computed utilizing the "Raster Calculator" feature within ArcGIS 10.8 (Zieg and Zawada, 2021, Inácio et al., 2023), as outlined in the preceding formulas. The resultant bitmaps were overlaid onto the delineated boundaries of the respective fields, which were generated using Google Earth Pro software. These overlays were subsequently exported as KML files and imported into ArcGIS 10.8 to facilitate statistical analysis, The "Band Collection Statistic" tool was employed, enabling a comprehensive multivariate analysis of the raster band collection. The analysis included the calculation of variance in relation to the mean, as well as the determination of the correlation coefficient, which illustrated the interrelationships among the data sets. In this study, For Sentinel2, The operational biophysical parameter products through the Sentinel Application Platform (SNAP) toolbox and produced through an ANN which has been trained by simulated spectra generated from well-known RTMs. The ESA offers robust OSRS software tailored for Sentinel data. You can download and set up the SNAP Toolbox (ESA 2018) on your personal computer by visiting http://step. esa. int/main/download/. It is available in both 32-bit and 64-bit formats. This toolbox includes a collection of visualization, analysis, and processing tools aimed at examining high-resolution optical S-2 and radar data.

2.8. Statistical analyses

This study utilized an analysis of variance (ANOVA) specifically designed for a split-plot arrangement within the framework of a randomized complete block design. In this arrangement, the main factor examined was the kind of micro-irrigation system used, with the blocks serving as the replicates. To identify statistically meaningful differences among the average groups revealed in the ANOVA, Duncan's least significant difference (LSD) test was applied, setting the significance level at a probability threshold of below 0.05. All statistical evaluations were carried out using the CO-STAT software (Stern, 1991). Furthermore, Pearson's correlation analysis and Heatmap visualization were executed through an online statistical analysis tool (Awad et al., 2024).

2.9. Feasibility study

The yearly overall expenditure was determined in accordance with (Anyaegbu et al., 2020) for the precision control system in the following manner, which is presented in the following equation (29):

$$\text{Annual total cost} = \text{Total fixed costs} + \text{Total variable costs} \quad (29)$$

The overall fixed expenditures (US$ y^{-1}) comprise costs associated with the control system, incorporating elements such as the electrical circuit board, Arduino, soil moisture sensors based on capacitance, solenoid valves, relays, adapters, memory cards, connecting wires, and installation, as well as any supplementary infrastructure. The overall variable expenses (US$ y^{-1}) are characterized as the aggregate of total operational expenditures, energy expenses, and maintenance costs. Estimated maintenance expenses are projected to be between 2.2% and 7.4% of the fixed expenditures (US$ y^{-1}) throughout a forecasted operational lifespan of 10 years.

3. Results

3.1. Irrigation water applied and irrigation water productivity

Throughout the experiment, the volume of irrigation water utilized across various microirrigation system treatments was maintained at a consistent level, with the objective of evaluating the impacts of different water application techniques that employed saline water and soil. Each treatment was allocated a uniform quantity of irrigation water, facilitating a comparative assessment of the

microirrigation systems based on their respective water application methods and the resulting effects on soil moisture, salinity distribution, and orange yield. This methodology not only contributes to the conservation of irrigation water but also guarantees adequate moisture for crop growth, alleviates plant stress, and ultimately enhances water productivity in conjunction with orange yields.

The irrigation water applied (IWA) for each micro-irrigation system was calculated following the procedures outlined in the Materials and Methods section, which considered the distribution efficiency of water application, leading to notable differences in the volumes of irrigation water applied to each system. In the first growing season, the T-tape (GR) treatment recorded the highest yield of 27.51 ton ha^{-1}, closely followed by the online PC dripper and Bubbler irrigation systems, which yielded 26.83 ton ha^{-1} and 24.07 ton ha^{-1}, respectively. Conversely, the mist sprayer treatment produced the lowest yield at 19.10 tons per hectare. The following growing season demonstrated a similar trend in orange productivity, with the T-tape(GR) again achieving a yield of 27.54 ton ha^{-1}, while the Bubbler and online PC dripper treatments yielded 27.54 ton ha^{-1} and 24.06 ton ha^{-1}, respectively. The mist sprayer continued to yield the least, at 18.09 ton ha^{-1}.

Regarding irrigation water productivity (IWP), the T-tape (GR) recorded an IWP of 6.08 kg m^{-3} in the first growing season, with the online PC dripper closely trailing at 5.37 kg m^{-3}. In sharp contrast, the RZWS demonstrated the lowest IWP, registering merely 3.12 kg m^{-3} in the second growing season. Notable differences in both yield and IWP were observed across all treatment methods.

Table 9. Effect of different microirrigation systems on yield, and water productivity.

Microirrigation system	Irrigation water applied (m^3 ha^{-1})		Productivity (ton ha^{-1})		IWP (kg m^{-3})	
	1st	2nd	1st	2nd	1st	2nd
T-tape (GR)	4521.48 d	5199.70 d	27.51 a	27.54 a	6.08 a	5.30 a
Online dripper	5140.42 a	5911.48 a	22.09 ab	22.49 ab	4.30 b	3.80 bc
Online PC dripper	4993.55 b	5742.58 b	26.83 a	24.06 a	5.37 ab	4.19 bc
Mist sprayers	4737.50 c	5448.12 c	19.10 b	18.09 bc	4.03 b	3.32 c
RZWS	4324.31 e	4972.95 e	21.22 ab	15.50 c	4.91 ab	3.12 c
Bubbler	5017.44 b	5770.06 b	24.07 ab	27.54 a	4.80 ab	4.77 ab

Means followed by different letters indicates significant differences between the treatments (n = 6; Duncan test at 95%).

3.2. Soil moisture distribution patterns

The distribution of soil moisture beneath micro-irrigation systems exhibited considerable variability; however, the most effective systems that achieved a consistent moisture distribution and reached a soil moisture level of 19% at a distance of at least 1.5 meters from the tree were identified as the T-tape (GR) dripper and the online PC dripper. In contrast, the moisture distribution was notably inconsistent across the various systems, with a marked reduction in moisture content observed under both RZWS and mist sprayers. Although mist sprayers deliver water in a manner akin to rainfall, the increase in temperature and wind speed contributed to a decline in the uniformity of moisture distribution and an escalation in evaporation losses, adversely impacting soil moisture levels (Fig. 3).

All drip irrigation systems effectively sustained elevated moisture levels in the vicinity of the root zone, yet differences in the diameter of the wetted areas were noted among the systems. The largest diameter of the wetting circle, which was recorded when the soil was at or near field capacity, was ranked from largest to smallest as follows: T-tape (GR) dripper, Online PC dripper, Bubbler, Online dripper, RZWS, and Mist sprayers. Furthermore, all systems demonstrated the highest concentration of salts at the edges of the wetted area, as depicted in Figure 3.

3.3. Salt distribution patterns

Figure (4) shows the effect of different micro irrigation systems on salts distribution patterns, where the disparity in the distribution and concentration of salts among various irrigation systems was significant, highlighting the intrinsic irregularity of salt distribution within the soil, both laterally and vertically. It was particularly noteworthy that the highest levels of salt concentration were recorded prior to irrigation in regions employing drip irrigation, which was implemented with a randomized treatment configuration to avoid interference from adjacent systems, including mist sprayers, RZWS, and bubblers systems **(Fig. 4)**.

Additionally, The most pronounced accumulation of salts was detected at the soil surface and within the upper soil strata, with a marked reduction in concentration observed as the depth of the soil increased. A comparative evaluation of the efficiency of salt removal before and after irrigation in drip irrigation systems indicated that the T-tape (GR) dripper demonstrated exceptional effectiveness, decreasing salt concentration from 1900 ppm to 800 ppm, which corresponds to a significant reduction of 1100 ppm at a horizontal distance of 1 meter from the tree and a depth of 0.50 meters (Fig. 4).

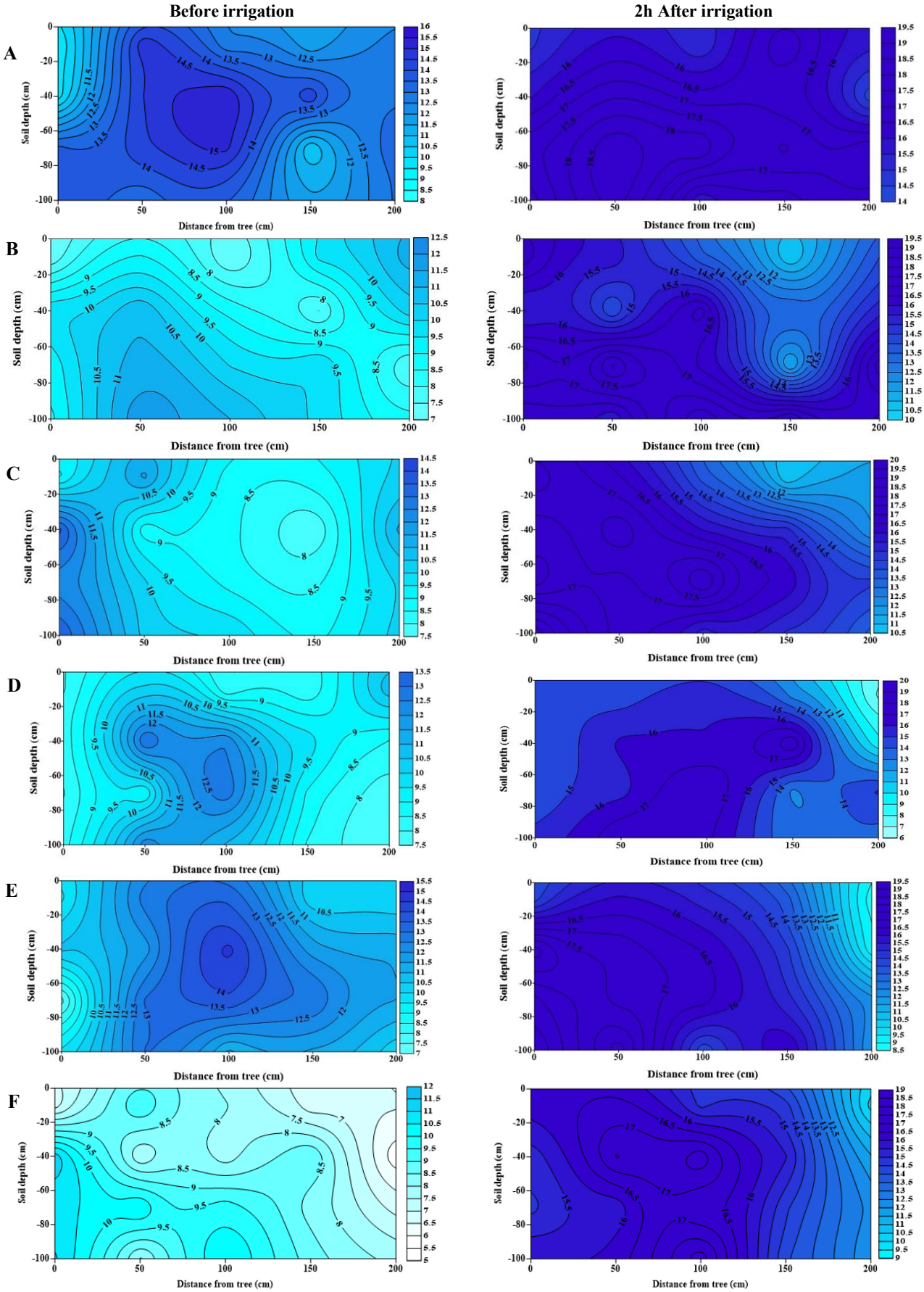

Fig. 3. Effect of different microirrigation systems on soil moisture content before and after irrigation as an average of both growing seasons, where A) T-tape GR dripper, B) Online dripper, C) Online PC dripper, D) Mist sprayer, E) RZWS, and F) Bubbler.

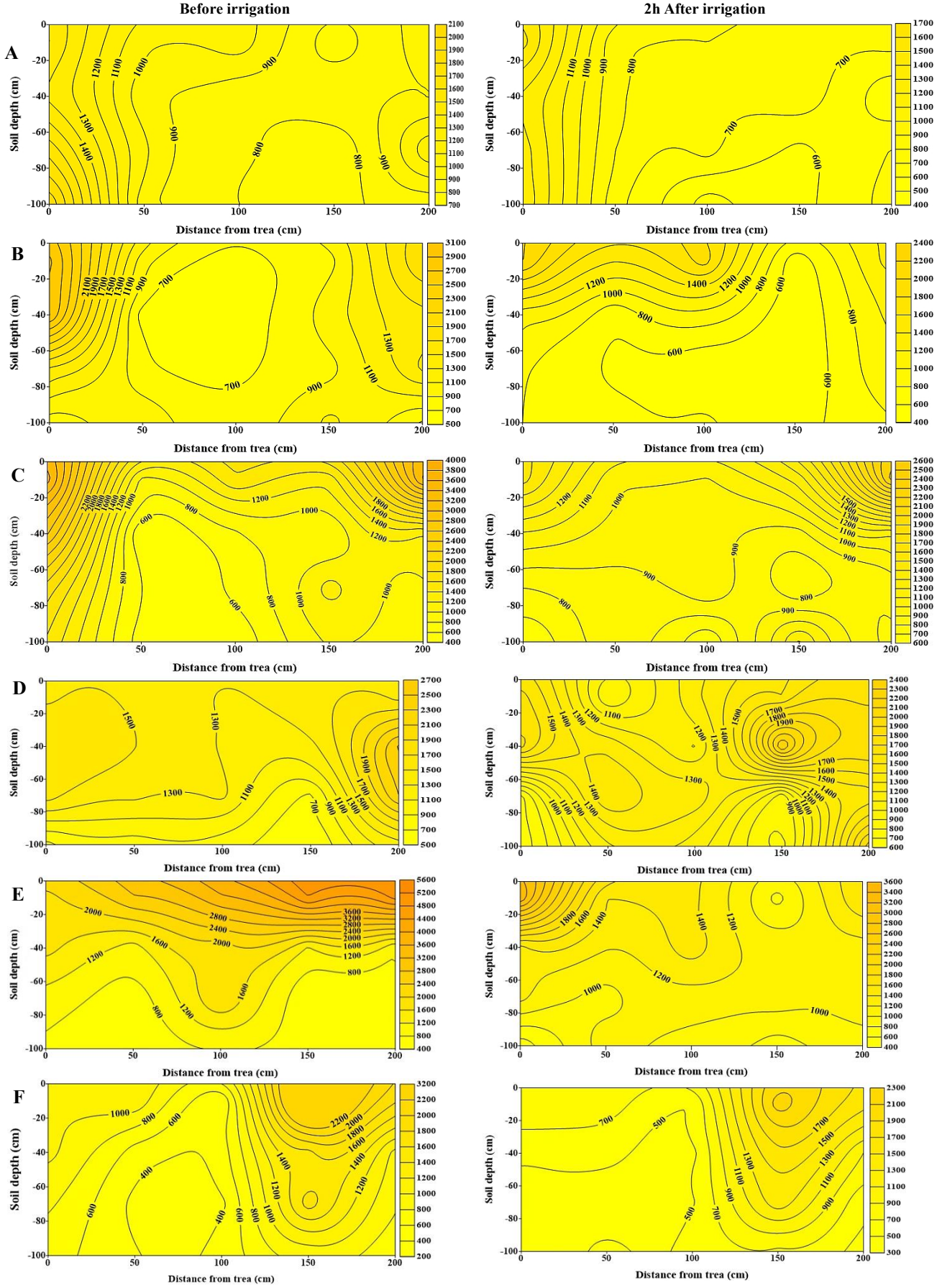

Fig. 4. Effect of different micro irrigation systems on salts distribution patterns before and after irrigation as an average of both growing seasons, where A) T-tape GR dripper, B) Online dripper, C) Online PC dripper, D) Mist sprayer, E) RZWS, and F) Bubbler.

3.4. Flowering and fruiting behavior

The mist sprayer demonstrated the highest initial fruit set during the first growing season, achieving a rate of 21.325%, while the Bubbler treatment followed closely with a rate of 19.916%. In contrast, the second growing season saw the RZWS treatment yielding the lowest initial fruit set at 8.520%. The final fruit set was maximized under the mist sprayers treatment, which recorded 9.050%, with the online dripper treatment at 7.900% during the second growing season. Conversely, the RZWS exhibited the lowest final fruit set of 1.681% in the first growing season (Table 10).

Regarding fruit drop, the Bubbler treatment resulted in the highest drop rate of 88.349, followed by the mist sprayer at 87.349 in the first growing season. The T-tape (GR) dripper achieved the highest flowering density of 27.700, with the Bubbler treatment at 20.250 in the first growing season. In the second growing season, the mist sprayers again recorded the lowest flowering density at 6.585. Additionally, the increase in the length of the main branch was greatest under the Bubbler and T-tape (GR) dripper treatments in the first growing season, with measurements of 36.724 and 30.219, respectively (Table 10).

Table 10. The effect of different microirrigation systems under saline irrigation water and soil on flowering and fruiting behavior of orange trees.

Microirrigation system	Initial fruit set (%)	Final fruit set (%)	Fruit drop (%)	Flowering density	The increase in length of main branch (%)
			2023-2024		
T-tape (GR)	11.357 b	4.988 ab	60.001 bc	27.700 a	30.219 ab
Online dripper	12.040 a	6.830 a	43.593 c	18.400 b	26.238 b
Online PC dripper	19.507 ab	3.804 ab	77.292 ab	13.930 c	12.896 c
Mist sprayers	21.325 a	2.603 b	87.349 a	9.700 d	6.803 c
RZWS	13.378 ab	1.681 b	84.287 a	19.533 b	28.473 b
Bubbler	19.916 ab	2.354 b	88.165 a	20.250 b	36.724 a
			2024-2025		
T-tape (GR)	20.203 b	2.652 cd	86.873 ad	22.520 a	20.530 ab
Online dripper	12.040 ab	7.900 cd	34.384 ab	19.563 c	13.620 bc
Online PC dripper	16.560 ab	3.989 b	75.912 c	20.252 b	17.560 abc
Mist sprayers	21.325 a	9.050 a	57.561 d	6.565 f	2.520 c
RZWS	8.520 ab	2.000 c	64.789 bc	11.520 e	11.523 ab
Bubbler	16.020 ab	3.000 d	87.516 a	19.520 c	26.550 a

Means followed by different letters indicates significant differences between the treatments (n = 7; Duncan test at 95%).

3.5. Physical, mechanical, and chemical fruit properties

3.5.1. Physical fruit properties

The online PC drippers treatment demonstrated the highest fruit weight, with measurements of 228.643 g and 206.044 g during the first and second growing seasons, respectively. This was followed by the T-tape (GR) dripper, which achieved a weight of 208.605 g. Additionally, the online PC drippers also produced the longest fruit, measuring 7.717 cm in the first growing season. In contrast, the mist sprayers recorded the shortest lengths of 6.862 cm and 7.059 cm in the first and second growing seasons, respectively. The online PC drippers had the largest fruit diameter of 7.482 cm in the first growing season, followed by bubblers at 7.121 cm in the second season, whereas the mist sprayers had the smallest diameter of 6.382 cm in the first growing season (Table 11).

Table 11. The effect of different microirrigation systems under saline irrigation water and soil on fruit weight, fruit length, fruit diameter, rind ratio, and shape index of Valencia orange fruits.

Microirrigation system	Fruit Weight (g)	Fruit Length (cm)	Fruit Diameter (cm)	Rind ratio	shape index
			1th growing season		
T-tape (GR)	189.083 b	7.117 bc	6.915 b	27.077 a	97.243 a
Online dripper	208.605 ab	7.396 ab	7.070 ab	21.102 b	95.691 a
Online PC dripper	228.643 a	7.717 a	7.482 a	22.249 ab	96.977 a
Mist sprayers	149.619 c	6.862 c	6.382 c	22.583 ab	93.010 a
RZWS	202.552 ab	7.435 ab	7.111 ab	24.096 ab	95.621 a
Bubbler	196.543 b	7.376 abc	6.946 b	25.276 ab	94.200 a
			2nd growing season		
T-tape (GR)	193.137 ab	7.382 abc	6.919 abc	25.067 ab	93.736 a
Online dripper	188.689 ab	7.211 cd	6.772 dcb	25.085 ab	93.898 a
Online PC dripper	206.044 a	7.504 ab	6.973 ab	26.453 a	92.919 ab
Mist sprayers	180.178 b	7.059 d	6.580 d	25.363 ab	93.228 ab
RZWS	179.432 b	7.334 bc	6.724 cd	20.241 b	91.672 b
Bubbler	208.223 a	7.533 a	7.121 a	24.241 ab	94.547 a

Means followed by different letters indicates significant differences between the treatments (n = 7; Duncan test at 95%)

Table 12. The effect of different microirrigation systems under saline irrigation water and soil on rind thickness, mean geometrical diameter, fruit volume, rag percentage, and Juice percentage of orange fruits.

Microirrigation system	Rind Thickness (mm)	Mean geometrical diameter (mm)	Fruit Volume (mL)	RAG (%)	Juice (%)
			1th growing season		
T-tape (GR)	1.004 abc	6.972 b	155.333 ab	42.326 abc	36.731 cd
Online dripper	1.295 a	7.202 ab	135.000 ab	57.323 a	44.672 abc
Online PC dripper	1.378 a	7.574 a	175.740 a	62.537 a	49.971 a
Mist sprayers	0.611 c	6.564 c	88.867 b	19.722 c	33.894 b
RZWS	1.077 ab	7.226 ab	209.922 a	50.939 ab	41.823 bcd
Bubbler	0.838 bc	7.100 b	142.133 ab	34.255 bc	45.283 ab
			2nd growing season		
T-tape (GR)	0.989 ab	7.055 bc	179.933 ab	35.597 ab	43.429 a
Online dripper	0.947 ab	6.925 cd	181.733 ab	38.948 ab	40.020 a
Online PC dripper	0.869 abc	7.162 ab	189.933 a	47.424 ab	42.512 a
Mist sprayers	0.809 bc	6.763 d	167.133 b	17.372 b	45.422 a
RZWS	0.690 c	6.932 cd	170.339 ab	50.506 ab	35.815 a
Bubbler	0.998 a	7.266 a	185.857 ab	52.989 a	43.252 a

Means followed by different letters indicates significant differences between the treatments (n = 7; Duncan test at 95%).

During the initial growing season, the T-tape (GR) dripper exhibited the highest rind ratio of 27.077, while the bubblers recorded the lowest at 20.241 in the subsequent season. The T-tape (GR) dripper also achieved a peak shape index of 97.243 in the first season, whereas the RZWS had a minimum shape index of 91.672 in the second season (Table 12).

Regarding rind thickness, the online PC drippers had the largest measurement at 1.378 mm in the first season, closely followed by the online drippers at 1.295 mm. The online PC drippers treatment

produced the highest mean geometrical diameter of 7.574 mm in the first season, followed by the Bubbler at 7.266 mm in the second season, whereas the mist sprayers had the smallest mean geometrical diameter of 6.564 mm during the first season (Table 12). Additionally, the RZWS recorded the highest fruit volume of 209.922 mL in the first season, while the mist sprayers had the lowest volumes of 88.867 mL in the first seasons. The online PC dripper also achieved the highest RAG percent value of 62.537% in the first season, contrasting with the mist sprayers lowest value of 17.372% in the second season. Similarly, the online PC dripper reached the maximum juice percent value of 49.971% in the first season, while the mist sprayer recorded the lowest juice percent of 33.894% in the second season (refer to Table 12).

3.5.2. Mechanical properties of orange fruits

Figure (5) represents the effect of different irrigation systems on the mechanical properties where during the first growing season, the online dripper demonstrated the highest firmness value of 39.000 N, whereas the RZWS exhibited the lowest firmness value of 20.033 N in the second growing season. Conversely (Fig. 5A), the T-tape (GR) dripper achieved the maximum penetration value of 87.851 N in the first growing season, while the mist sprayers recorded a minimum value of 55.551 N in the second growing season (Fig. 5B).

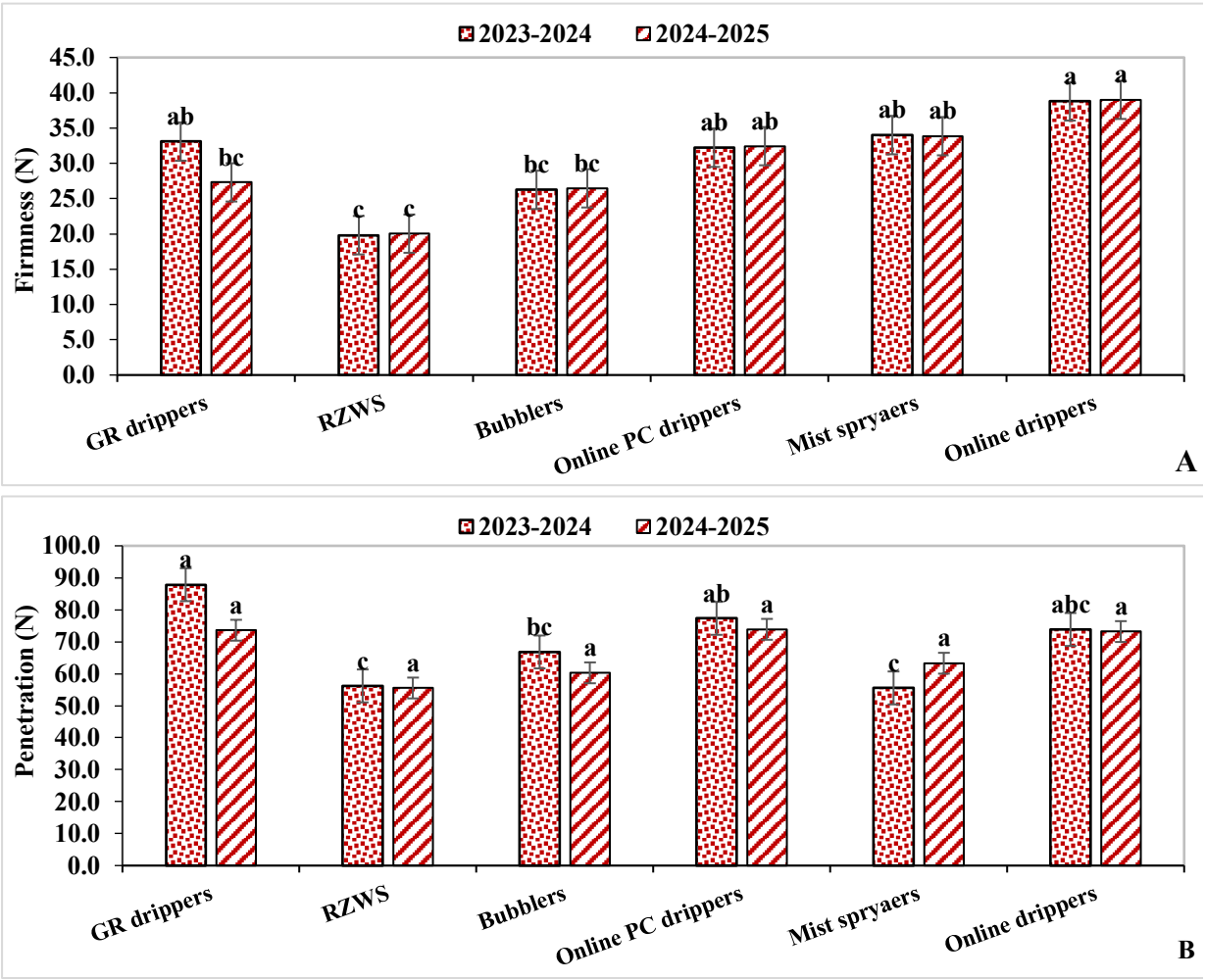

Fig. 5. Effect of different irrigation systems on the mechanical properties of orange fruits, where A) Firmness and B) Penetration.

3.5.3. Chemical fruit properties

The mist sprayer treatment demonstrated the highest total soluble solids (TSS) of 13.333% and 13.233% during the first and second growing seasons, respectively. In contrast, the T-tape (GR) exhibited the lowest TSS values of 11.667% and 11.167% in the first and second growing seasons, respectively. Additionally, the mist sprayer recorded the highest acidity level of 0.939% in the first growing season, while the lowest acidity was noted at 0.572% in the second growing season (Table 13).

The mist sprayer also revealed the highest TSS/acidity ratio of 23.580 in the second growing season, whereas the online dripper had the lowest ratio of 15.689 during the same period. Furthermore, the mist sprayer achieved the highest pH value of 3.420 in the first growing season, while the RZWS treatment recorded the lowest pH of 3.140 in the second growing season. The Bubbler treatment

indicated the highest phenolic content of 0.186% in the first growing season, whereas the online PC dripper showed the lowest phenolic value of 0.165% in the second growing season. The online PC dripper also attained the highest carotenoid content of 0.278 g per 100 g in the first growing season, while the online dripper had the lowest carotenoid value of 0.148 g per 100 g in the second growing season (Table 13).

Moreover, the online PC dripper exhibited the highest vitamin C content of 29.755 mg per 100 g in the first growing season, while the RZWS treatment recorded the lowest vitamin C value of 56.100 mg per 100 g in the second growing season. The RZWS treatment achieved the maximum total sugar content of 1.914 mg per 100 g in the first growing season, while the T-tape (GR) recorded the lowest total sugar value of 2.234 mg per 100 g in the second growing season. Lastly, the T-tape (GR) reached the highest DPPH value of 48.561% in the first growing season, while the bubbler treatment noted the lowest DPPH value of 50.316% in the second season (Table 13).

3.6. Vegetative growth

Figure (6) represents the effect of different microirrigation systems on vegetative growth where during the first growing season, the T-tape (GR) achieved the highest leaf area measurement of 32.888 cm², whereas the RZWS recorded the lowest at 22.363 cm² in the second growing season. In contrast, the mist sprayers demonstrated the highest leaf moisture content of 56.379% during the first growing season, while the Bubbler had the lowest leaf moisture content of 51.553% in the second growing season. Additionally, the mist sprayer showed the greatest leaf moisture loss of 97.1% in the first growing season, compared to the Bubbler, which recorded the least moisture loss at 82.424% in the second growing season (Fig. 6).
Furthermore, the T-tape (GR) exhibited the highest skin moisture content of 88.774% in the first growing season, while the online dripper had the lowest skin moisture content of 70.029% in the second growing season. Notably, the online PC dripper reached the highest leaf chlorophyll value of 71.575 SPAD in the second growing season, whereas the mist sprayer recorded the lowest leaf chlorophyll value of 46.328 SPAD during the same period (Fig. 6).

Table 13. The chemical fruit properties for both growing seasons under different microirrigation systems treatments.

Microirrigation system	TSS (%)	Acidity (%)	TSS/Acidity ratio	pH	Phenolic (%)	Carotenoid (g 100 g^{-1})	Vitamin C (mg 100 g^{-1})	Total sugar (%)	DPPH (%)
1th growing season									
T-tape (GR)	11.667 c	0.683 b	17.514 a	3.190 c	0.168 d	0.144 e	25.378 b	1.434 b	48.561 a
Online dripper	13.167 bc	0.747ab	18.245 a	3.340 bc	0.184 b	0.150 d	23.102 c	1.551 b	32.203 f
Online PC dripper	12.375 bc	0.768 ab	16.242 a	3.300 bc	0.148 c	0.278 a	29.755 a	1.537 b	47.402 d
Mist sprayers	13.333 abc	0.939a	14.261 a	3.420 abc	0.143 f	0.130 f	26.593 b	1.434 b	37.560 e
RZWS	12.750 bc	0.789 ab	16.294 a	3.160 bc	0.172 c	0.171 b	18.755 d	1.914 a	41.020 d
Bubbler	12.500 ab	0.896ab	14.089 a	3.400 ab	0.186 a	0.157 c	19.577 d	1.465 b	45.580 c
2nd growing season									
T-tape (GR)	11.167 b	0.674 ab	16.602 b	3.170 e	0.198 c	0.161 bc	60.775 d	2.234 f	55.368 bc
Online dripper	12.233 ab	0.789a	15.689 b	3.360 c	0.205 b	0.148 c	67.780 a	2.366 e	55.158 bc
Online PC dripper	11.733 ab	0.640 ab	18.545 ab	3.320 d	0.165 f	0.220 abc	58.438 e	4.852 a	63.368 a
Mist sprayers	13.233 b	0.572b	23.580 a	3.440 b	0.178 e	0.208 bc	61.710 b	3.404 c	53.053 bc
RZWS	12.367 ab	0.704ab	18.010 ab	3.140 e	0.182 d	0.302 a	56.100 f	3.197 d	57.895 ab
Bubbler	11.267 b	0.591 b	19.204 ab	3.480 a	0.220 a	0.238 ab	61.243 c	4.492 b	50.316 c

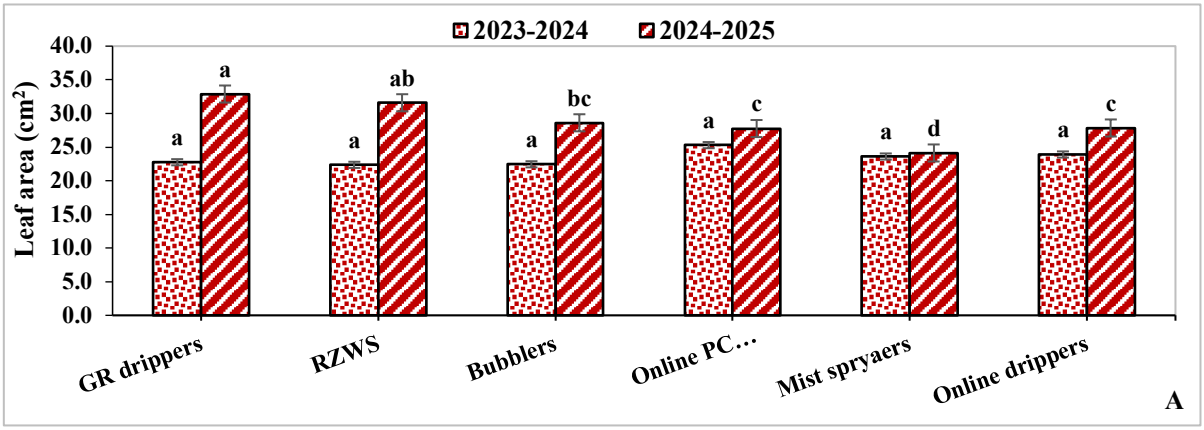
2023-2024
2024-2025
Leaf area (cm²)
40.0
35.0
30.0
25.0
20.0
15.0
10.0
5.0
0.0
a a
a ab
a bc
a c
a d
a c
GR drippers
RZWS
Bubblers
Online PC…
Mist spryaers
Online drippers
A

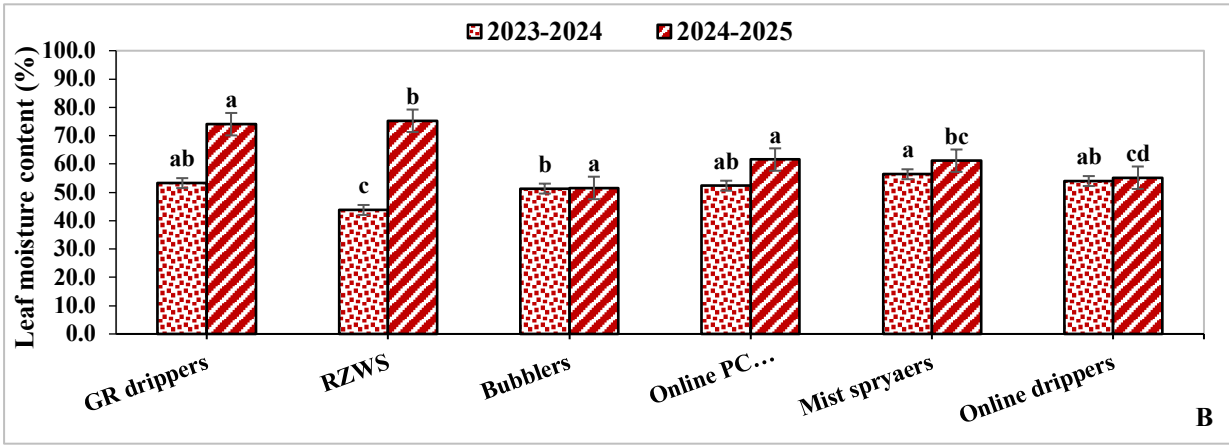
2023-2024
2024-2025
Leaf moisture content (%)
100.0
90.0
80.0
70.0
60.0
50.0
40.0
30.0
20.0
10.0
0.0
ab a
c b
b a
ab a
a bc
ab cd
GR drippers
RZWS
Bubblers
Online PC…
Mist spryaers
Online drippers
B

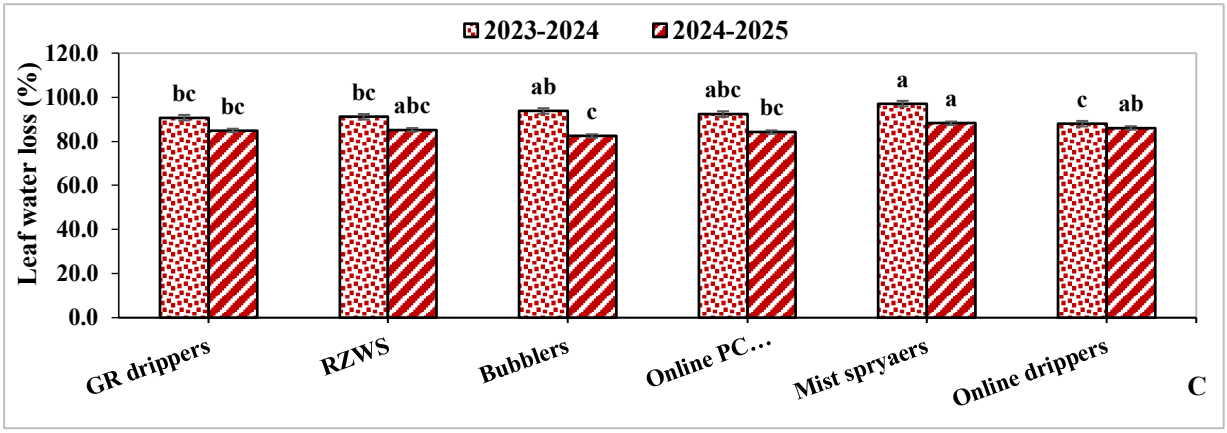
2023-2024
2024-2025
Leaf water loss (%)
120.0
100.0
80.0
60.0
40.0
20.0
0.0
bc bc
bc abc
ab c
abc bc
a a
c ab
GR drippers
RZWS
Bubblers
Online PC…
Mist spryaers
Online drippers
C

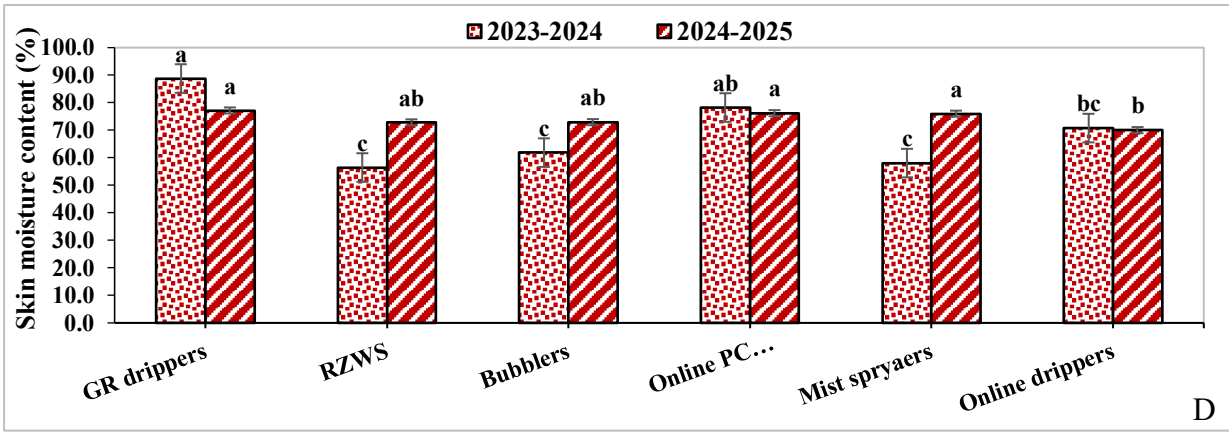
2023-2024
2024-2025
Skin moisture content (%)
100.0
90.0
80.0
70.0
60.0
50.0
40.0
30.0
20.0
10.0
0.0
a a
c ab
c ab
ab a
c a
bc b
GR drippers
RZWS
Bubblers
Online PC…
Mist spryaers
Online drippers
D

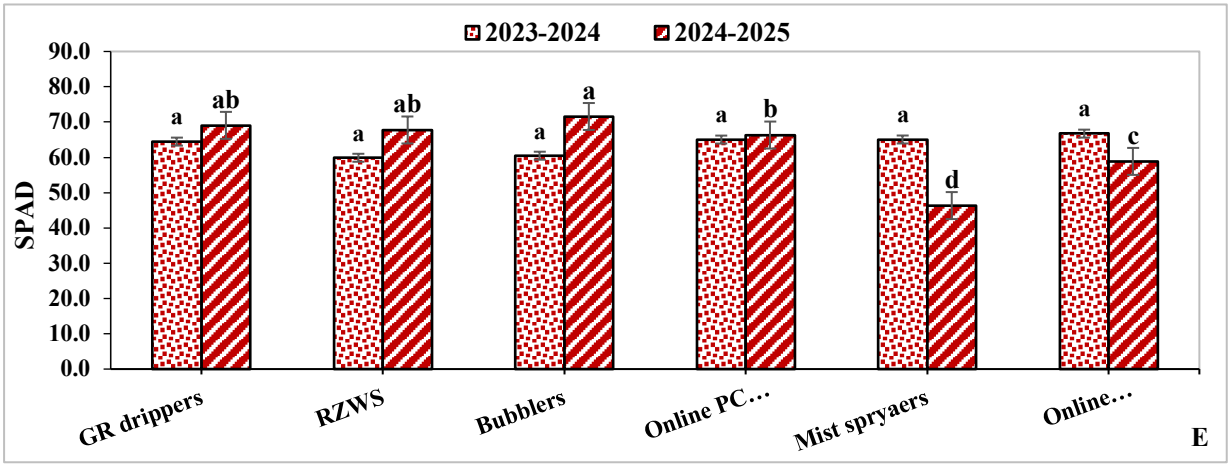

Fig. 6. The effect of different microirrigation systems under saline irrigation water and soil on leaf area, leaf moisture content, leaf moisture losses, skin moisture content and leaf chlorophyll (SPAD) of orange fruit, where A) Leaf area, B) Leaf moisture content, C) Leaf water loss, D) Skin moisture content and E) SPAD.

Means followed by the different letters within each column significantly differ according to the Duncan multiple comparison test at the 5% level.

Each value is the average of three replicates for each growing season.

3.7. Leaf nutrient contents

The Online PC dripper treatment yielded the highest leaf nitrogen content (N) at 2.278% during the second growing season, followed by the online dripper at 2.207%. In contrast, the lowest leaf nitrogen content was recorded under the online dripper at 1.624% during the first growing season. The online PC dripper treatment yielded the highest leaf phosphorus content (P) at 0.589% and 0.409% in the 1th and 2nd growing seasons, respectively. On the other hand, the RZWS treatment recorded the lowest value of 0.109% in the 2nd growing season (Table 14).

The online PC dripper treatment exhibited the highest leaf potassium content (K) in the second growing season at 1.192%, with the Bubbler system close behind at 1.183%. The mist sprayer treatment recorded the lowest potassium content in the first growing season at 0.826%. In terms of sodium content (Na), the Bubbler treatment had the highest levels in the second growing season at 0.412%, followed by the online PC dripper at 0.313%. In contrast, the lowest leaf sodium content was recorded under the Bubbler at 0.232% during the first growing season. The online PC dripper treatment had the highest leaf calcium content (Ca) at 1.517 g 100 g^{-1} during the 2nd growing season, followed by the Bubbler at 0.427 g 100 g^{-1}. In contrast, the lowest leaf calcium content was recorded under the online dripper treatment at 1.115 g 100 g^{-1} during the first growing season. The online dripper treatment displayed the maximum proline, measuring 59.547 mg 100 g^{-1} and 49.189 mg 100 g^{-1} in the 1th and 2nd growing seasons, respectively. On the other hand, the T-tape (GR) recorded the lowest value of 16.095 mg 100 g^{-1} in the 2nd growing season (Table 14).

Table 14. The effect of different microirrigation systems under saline water and soil on leaf nutrient content of orange trees.

Microirrigation system	N (%)		P (%)		K (%)		Na (%)		Ca (g 100 g^{-1})		Proline (mg 100 g^{-1})	
	1st	2nd	1st	2nd	1st	2nd	1st	2nd	1st	2nd	1st	2nd
T-tape (GR)	2.022ab	2.168c	0.513b	0.116e	1.073d	0.907e	0.368a	0.236e	1.759a	0.338d	54.351 b	16.095 f
Online dripper	1.624b	2.207b	0.253e	0.134d	1.233c	0.965f	0.283e	0.237d	1.115c	0.304e	59.547 a	49.189 a
Online PC dripper	1.751b	2.278a	0.589a	0.409a	1.280b	1.192a	0.366b	0.313b	1.589ab	1.517a	54.050 c	21.749 d
Mist sprayers	2.273a	1.870f	0.236f	0.267b	0.826f	1.026c	0.353c	0.263c	1.498b	0.420c	46.057 f	21.459 e
RZWS	2.011ab	2.142d	0.297d	0.109f	1.440a	1.007d	0.318d	0.183f	1.216c	0.265f	54.049 d	45.563 b
Bubbler	1.962ab	1.986e	0.345c	0.157c	1.002e	1.183b	0.232f	0.412a	1.266c	0.427b	53.779 e	22.554 e

Means followed by different letters indicates significant differences between the treatments (n = 6; Duncan test at 95%).

3.8. Remote sensing indices

3.8.1. Performance of micro-irrigation systems on vegetation parameters

Microirrigation systems are essential for mitigating salinity stress and enhancing the health of orange crops. The study revealed significant differences in the effectiveness of various microirrigation systems, with advanced options such as online drippers and mist sprayers consistently outperforming bubblers.

Figure (7) monitors the effect of different microirrigation systems on soil salinity and vegetative growth through remote sensing indices, where the brightness index (BI), which evaluates the salt and organic matter content at the soil surface, showed notable variation across the irrigation systems. As depicted in Figure (7A), mist sprayers and online drippers recorded the highest BI values, averaging 0.185 ± 0.004 and 0.180 ± 0.005, respectively, indicating healthier vegetation and improved stress management. In contrast, the RZWS system exhibited the lowest BI values (mean = 0.167 ± 0.005).

Figure (7A) illustrates a significant positive correlation ($r = 0.421$, $p < 0.001$) between BI and SI-Normalized. The infrared percentage vegetation index (IPVI), which measures vegetation vitality, also displayed significant differences among the irrigation systems. As shown in Figure (7B), RZWS and Online PC drippers achieved the highest IPVI values, with means of 0.647 ± 0.004 and 0.643 ± 0.004, respectively, indicating healthier vegetation and better stress management. Conversely, T-tape GR recorded the lowest IPVI values (mean = 0.623 ± 0.003).

Figure (7B) reveals a significant negative correlation ($r = -0.100$, $p < 0.001$) between IPVI and SI-Normalized. The green normalized difference vegetation index (GNDVI), which also assesses vegetation vitality, showed significant variation among the irrigation systems. As illustrated in Figure 7C, RZWS and Online PC drippers achieved the highest GNDVI values, averaging 0.364 ± 0.008 and 0.353 ± 0.008, respectively, indicating healthier vegetation and improved stress management. In contrast, mist sprayers recorded the lowest GNDVI values (mean = 0.325 ± 0.006). Figure (7C) illustrates a notable positive correlation ($r = 0.117$, $p < 0.001$) between the GNDVI and SI-Normalized.

The normalized difference vegetation index (NDVI), which evaluates the health and density of vegetation, showed considerable differences across various irrigation systems. As depicted in Figure (7D), the RZWS recorded the highest NDVI values (mean = 0.293 ± 0.009), indicating improved vegetation health and better stress management.

In contrast, T-tape GR exhibited the lowest NDVI values (mean = 0.244 ± 0.006), reflecting its insufficient efficacy in mitigating salinity issues. This finding is corroborated by Figure (8D), which illustrates a notable negative correlation ($r = -0.092$, $p < 0.001$) between NDVI and the normalized salinity index (SI-Normalized). The decline in NDVI corresponding with increased salinity levels emphasizes the importance of implementing effective irrigation strategies to preserve crop productivity.

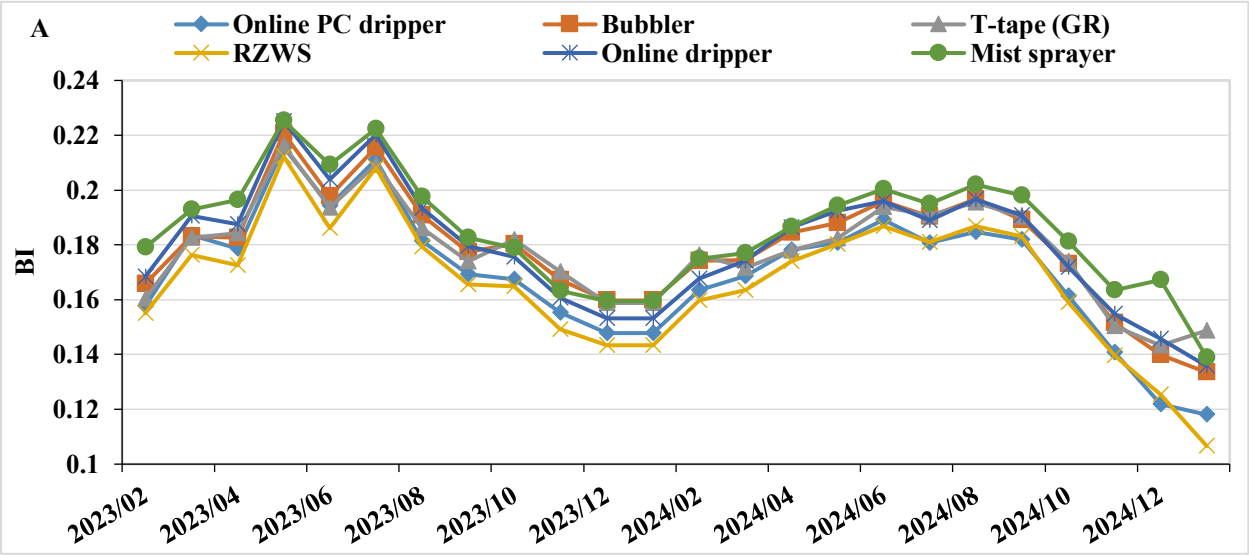

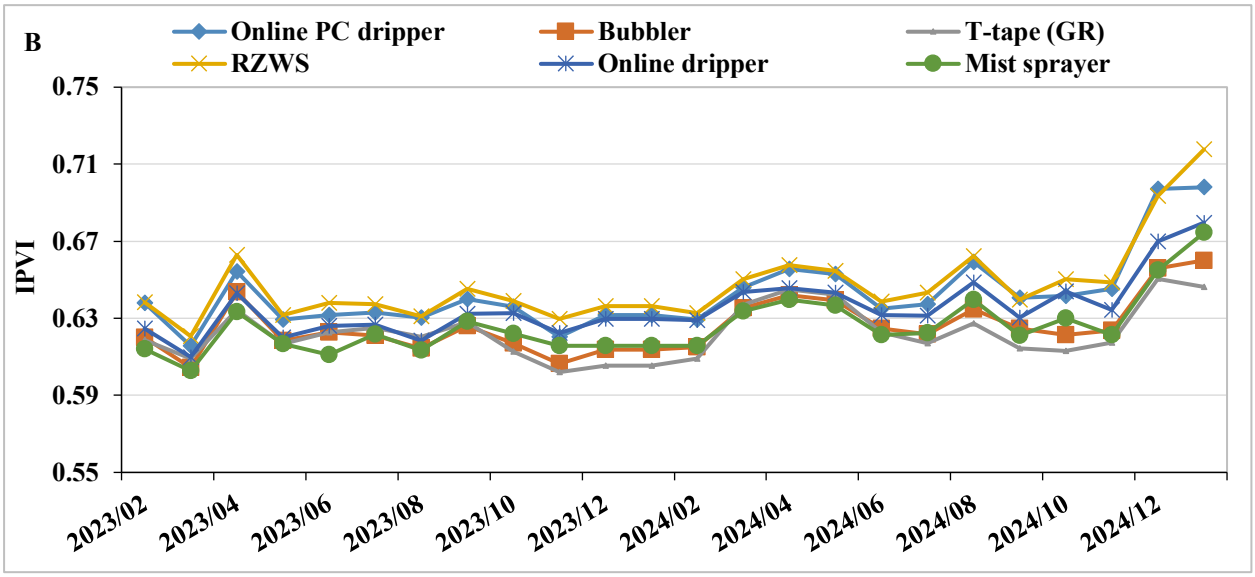
B
Online PC dripper
Bubbler
T-tape (GR)
RZWS
Online dripper
Mist sprayer
IPVI
0.75
0.71
0.67
0.63
0.59
0.55
2023/02
2023/04
2023/06
2023/08
2023/10
2023/12
2024/02
2024/04
2024/06
2024/08
2024/10
2024/12

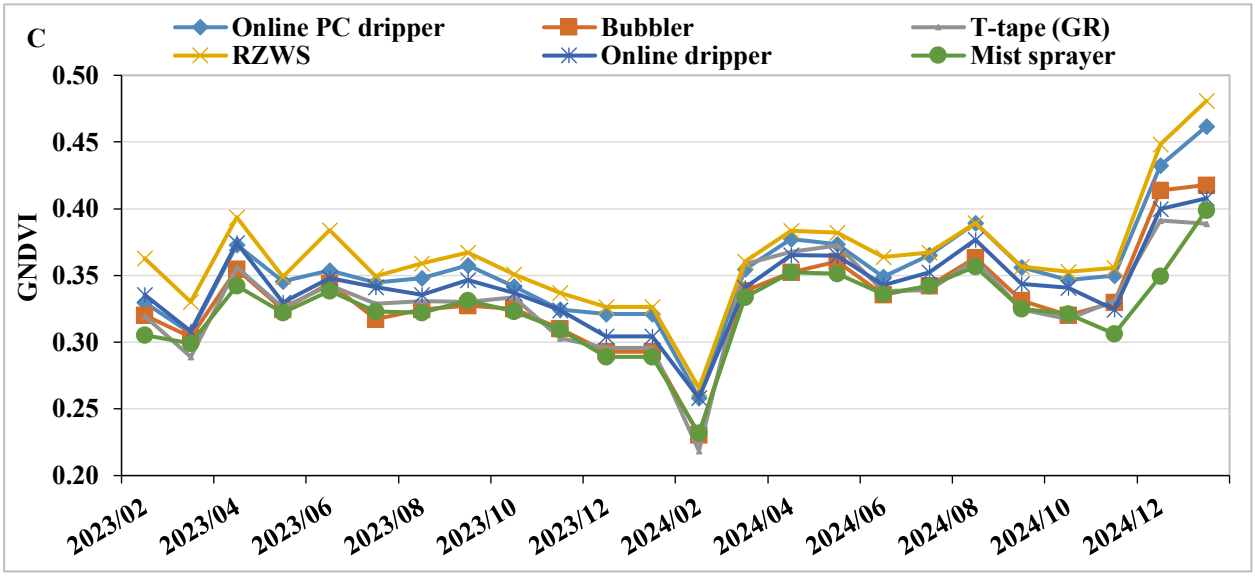
C
Online PC dripper
Bubbler
T-tape (GR)
RZWS
Online dripper
Mist sprayer
GNDVI
0.50
0.45
0.40
0.35
0.30
0.25
0.20
2023/02
2023/04
2023/06
2023/08
2023/10
2023/12
2024/02
2024/04
2024/06
2024/08
2024/10
2024/12

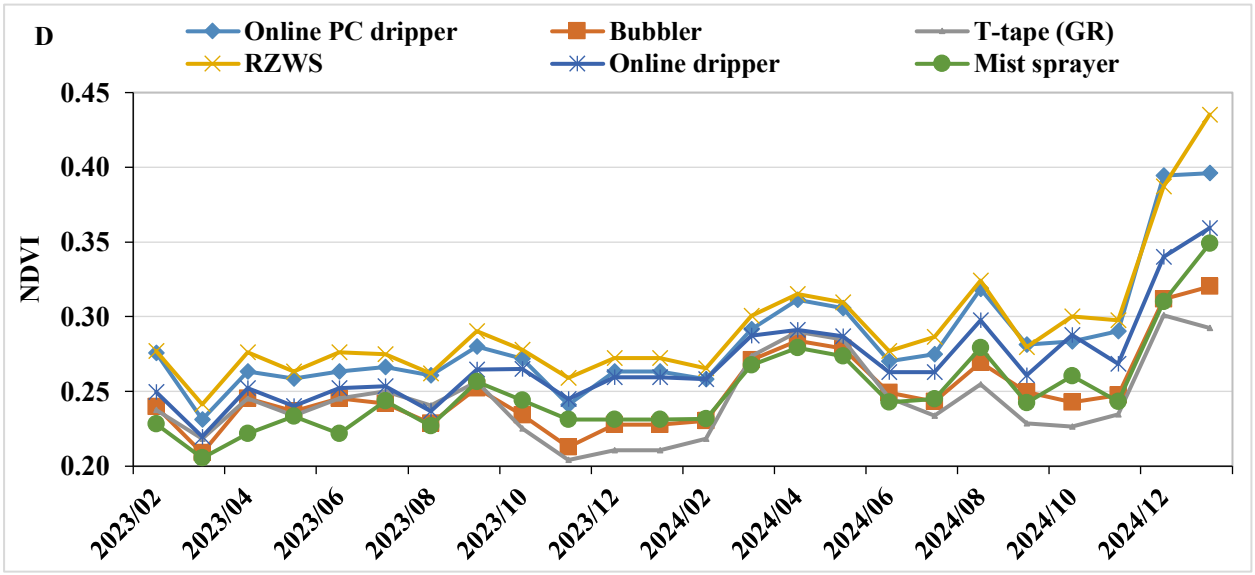
D
Online PC dripper
Bubbler
T-tape (GR)
RZWS
Online dripper
Mist sprayer
NDVI
0.45
0.40
0.35
0.30
0.25
0.20
2023/02
2023/04
2023/06
2023/08
2023/10
2023/12
2024/02
2024/04
2024/06
2024/08
2024/10
2024/12

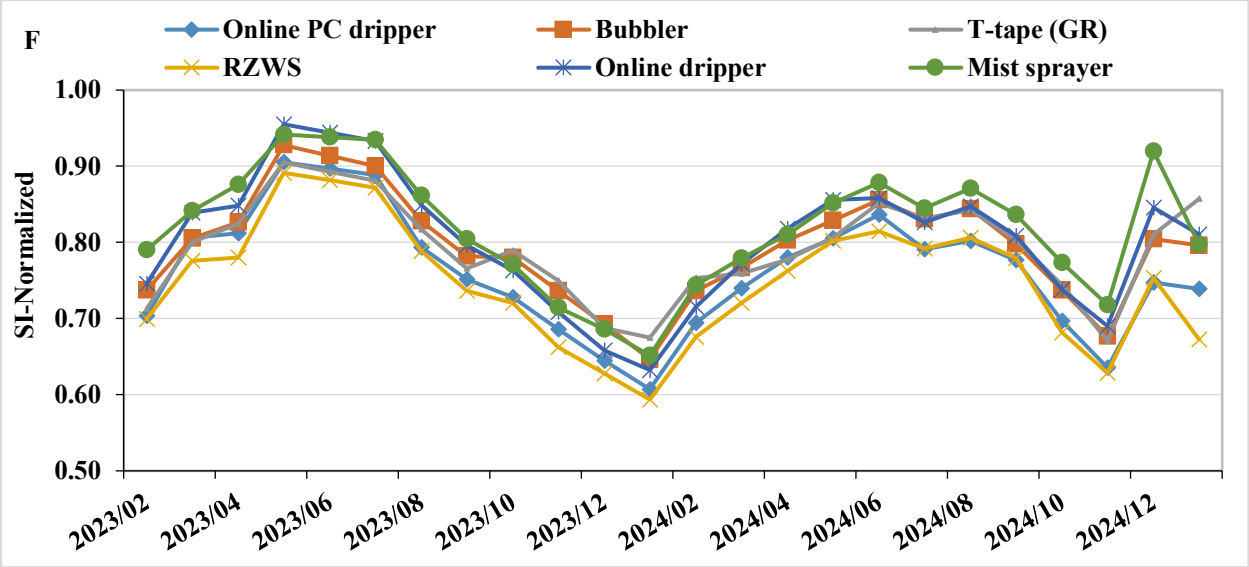

Fig. 7. The temporal variation of the BI, IPVI, GNDVI, NDVI, and SI-Normalized over the both growing seasons under different microirrigation systems.

Additionally, trends in salinity stress over time further underscore the benefits of sophisticated irrigation systems. Online drippers demonstrated the highest salinity stress levels (mean SI-Normalized = 0.979 ± 0.184), whereas online PC drippers exhibited significantly lower and more consistent salinity levels (mean SI-Normalized ≈ 0.745 ± 0.018). This consistency is vital for ensuring the long-term health and productivity of vegetation (Fig. 7F).

3.8.2. Temporal analysis of vegetation health and salinity stress

Temporal fluctuations in vegetation indices provided significant insights into how orange trees adapt to salinity stress. The Normalized Difference Vegetation Index (NDVI) and Brightness Index (BI) exhibited consistent performance across various advanced irrigation systems throughout the study duration. Online drippers consistently recorded higher NDVI values, reflecting their effectiveness in maintaining a healthy canopy density (Fig. 7D).
Similarly, mist sprayers achieved superior BI values, indicating their capability in managing stress conditions effectively (Fig. 7A). The observed trends related to salinity stress highlighted considerable temporal variations among the different irrigation systems. Online PC drippers successfully sustained stable salinity levels, demonstrating their precision in water distribution and salinity control. In contrast, bubblers exhibited fluctuating and elevated salinity stress levels, emphasizing the need for improved irrigation strategies within these systems (Fig. 7F).

3.8.3. Relationships between salinity and vegetation indices

The relationships between salinity and vegetation indices is represented in figure (8). The online PC dripper irrigation system consistently achieved higher NDVI values compared to other systems, indicating its superior ability to mitigate salinity stress and enhance vegetation health. In contrast, the T-tape (GR) system produced lower NDVI values, suggesting insufficient water distribution and ineffective salinity management. Additionally, the BI demonstrated a significant positive correlation with salinity indices ($r = 0.421$, $p < 0.001$) (Fig. 8A), indicating that changes in the salt and organic matter content of the soil surface are adaptive responses to salinity stress.
Among the various indices assessed, the Normalized Difference Vegetation Index (NDVI) and Brightness Index (BI) exhibited the strongest correlations with salinity metrics, thereby validating their roles as key indicators of vegetation health and resilience to stress. The NDVI showed a significant negative correlation with the SI-Normalized ($r = -0.092$, $p < 0.001$) (Fig. 8E), highlighting the adverse effects of salinity on plant health, where increased salinity levels are associated with reduced vegetation vigor and lower canopy density.
The increase in BI with higher salinity levels reflects physiological adaptations in vegetation. Among the irrigation techniques, online drippers and bubblers recorded the highest BI values, emphasizing their effectiveness in facilitating stress adaptation and preserving pigment stability in saline conditions.

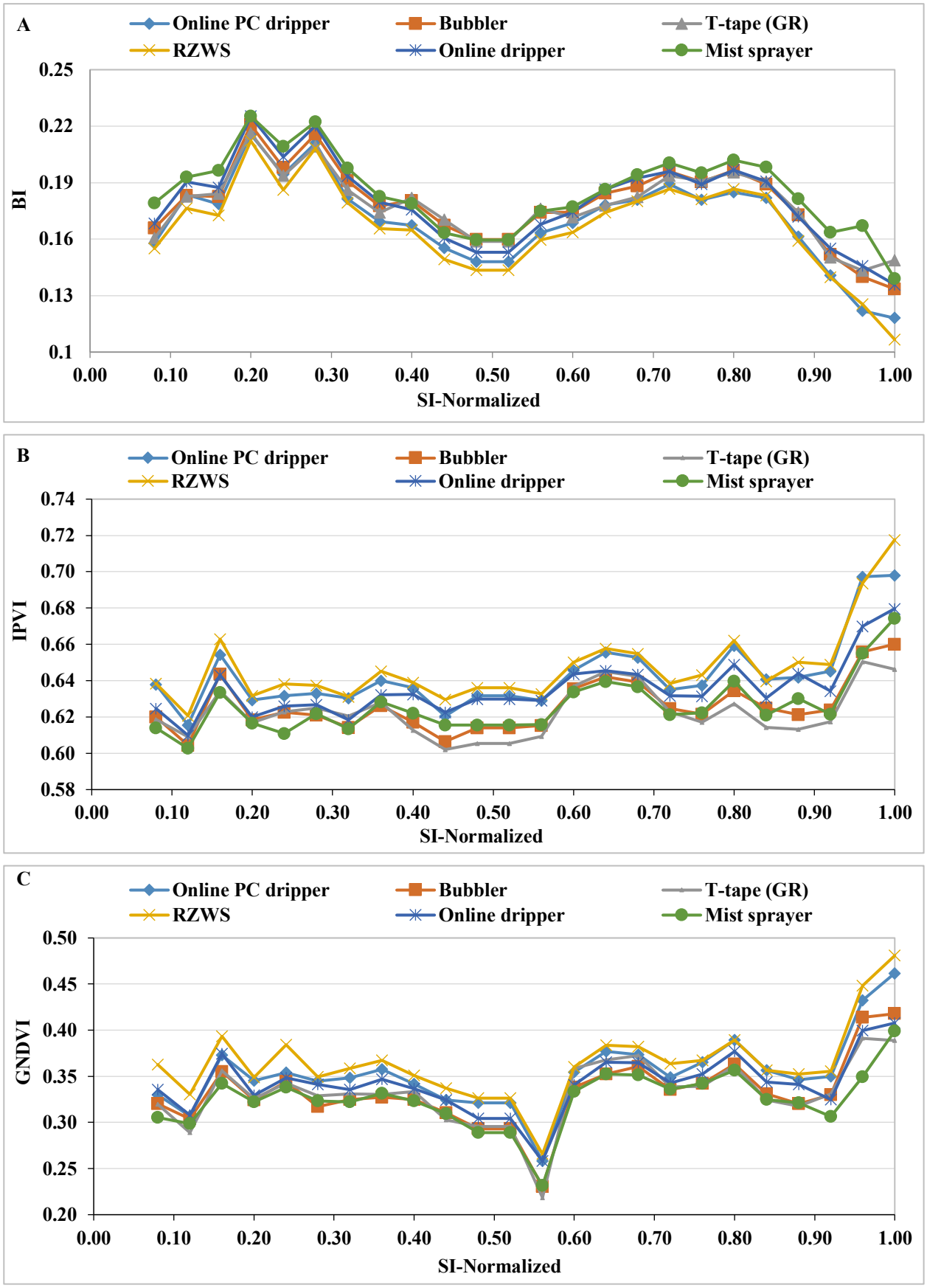
A
Online PC dripper
Bubbler
T-tape (GR)
RZWS
Online dripper
Mist sprayer
BI
0.25
0.22
0.19
0.16
0.13
0.1
0.00 0.10 0.20 0.30 0.40 0.50 0.60 0.70 0.80 0.90 1.00
SI-Normalized
B
Online PC dripper
Bubbler
T-tape (GR)
RZWS
Online dripper
Mist sprayer
IPVI
0.74
0.72
0.70
0.68
0.66
0.64
0.62
0.60
0.58
0.00 0.10 0.20 0.30 0.40 0.50 0.60 0.70 0.80 0.90 1.00
SI-Normalized
C
Online PC dripper
Bubbler
T-tape (GR)
RZWS
Online dripper
Mist sprayer
GNDVI
0.50
0.45
0.40
0.35
0.30
0.25
0.20
0.00 0.10 0.20 0.30 0.40 0.50 0.60 0.70 0.80 0.90 1.00
SI-Normalized

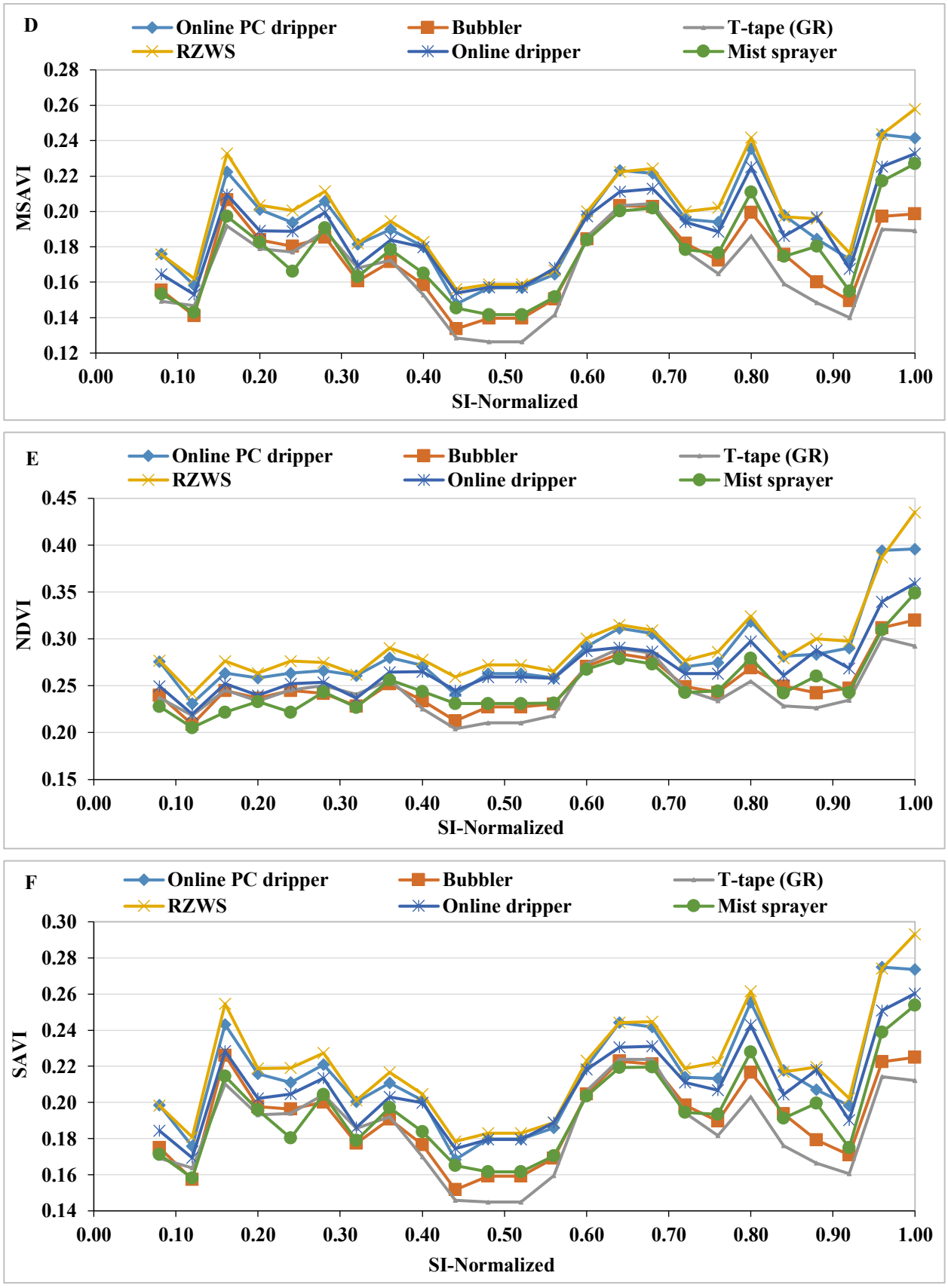

Fig. 8. The relationships between salinity and vegetation indices over the both growing seasons under different microirrigation systems, where A) SI-Normalized and BI, B) SI-Normalized and IPVI, and C) SI-Normalized and GNDVI, D) SI-Normalized and MSAVI, and E) SI-Normalized and NDVI F) SI-Normalized and SAVI.

Other indices offered supplementary insights into vegetation responses to salinity, although with weaker correlations than NDVI and BI (Figs. 8B, D, F). For instance, the GNDVI displayed a modest positive correlation with salinity (r = 0.117), as shown in Figure (8C), suggesting limited changes in chlorophyll content under salinity stress, which indicates that GNDVI may serve as a secondary indicator of vegetation health.

3.9. Cluster analysis and Correlation study

The two-way cluster analysis (Fig. 9), accompanied by the corresponding Dendrogram derived from various microirrigation systems, revealed that the Dendrogram pertaining to vegetative growth, quality metrics, remote sensing, and irrigation parameters is organized into three distinct categories (Fig. 9). This analysis, which is based on 40 measurements, classified the data into four groups designated as A, B, C, and D, while the microirrigation system treatments were grouped into three categories: drop irrigation (Group A), rain irrigation (Group B), and bubble irrigation (Group C) (Fig. 9).

Additionally, each of these three groups (A, B, and C) is further subdivided into two to three subcategories. Group A includes T-tape GR drippers (A-1), online drippers (A-2), and online PC drippers (A-3). In a similar manner, Group B encompasses mist sprayers (B), whereas Group C consists of RZWS (C-1) and bubblers (C-2). The analysis employs red to indicate a positive impact and blue to represent a negative impact. The results from the two-way cluster analysis indicated that the online dripper (A-2) and online PC dripper (A-3) treatments had a beneficial effect on the parameters studied, including IWP, yield, NDVI, MSAVI, SAVI, SI, SIPI, LAI, chlorophyll, and carotenoids. In contrast, the mist sprayer (B), RZWS (C-1), and bubbler (C-2) treatments demonstrated more adverse effects on all measured parameters (Fig. 9).

The analysis conducted using Pearson's correlation method aimed to assess the interrelationships, both positive and negative, among the various parameters under investigation (Fig. 10). The results indicated a robust positive correlation between irrigation water productivity (IWP) and multiple parameters, which were ranked in descending order of correlation strength: Productivity (0.87), flowering density (0.76), Aspect ratio (0.61), Penetration (0.55), Leaf chlorophyll (0.54), P (0.54), Na (0.51), Fruit width (0.51), Ca (0.50), and Yield (0.49). In contrast, a significant negative correlation was identified between IWP and MSAVI (-0.62), along with other parameters such as SAVI (-0.60), IPVI (-0.53), NDVI (-0.53), Vitamin C (-0.40), TSS/Acidity (-0.37), GNDVI (-0.36), Total sugar (-0.35), Leaf area and IWA (-0.33), and Leaf moisture content (-0.31), as depicted in Fig. 10.

3.10. Feasibility study

An economic evaluation of different microirrigation systems indicated that the T-tape (GR) dripper treatment generated the highest net farm income, with fixed costs (FC) recorded at 1262.41 US$ per year and variable costs (VC) amounting to 1450.84 US$ per year. As a result, the total annual costs (TC) reached 2713.26 US$ per year, while the total revenue (TR) was noted at 11010.0 US$ per year, based on an average orange price in Egypt for 2024 estimated at 400 US$ per ton, translating to a price of 0.4 US$ per kilogram. This led to a net farm income (NFI) of 8296.74 US$ per year for the T-tape GR system, followed by the Bubbler and online PC dripper systems, which yielded net farm incomes of 7568.98 US$ per year and 7437.07 US$ per year, respectively (Table 15).

These results highlight the benefits of microirrigation systems, especially drip irrigation, in fostering sustainable water management practices. Such systems are particularly advantageous in areas grappling with irrigation water salinity and soil salinity challenges, offering farmers a lucrative return. The ongoing adoption of these irrigation techniques is crucial for the preservation of essential water resources for agricultural production. Drip irrigation not only conserves water but also alleviates the negative impacts of salinity on crops by reducing soil evaporation and keeping salt concentrations away from the root zone, while simultaneously curbing weed growth, thus improving the productivity of orange trees.

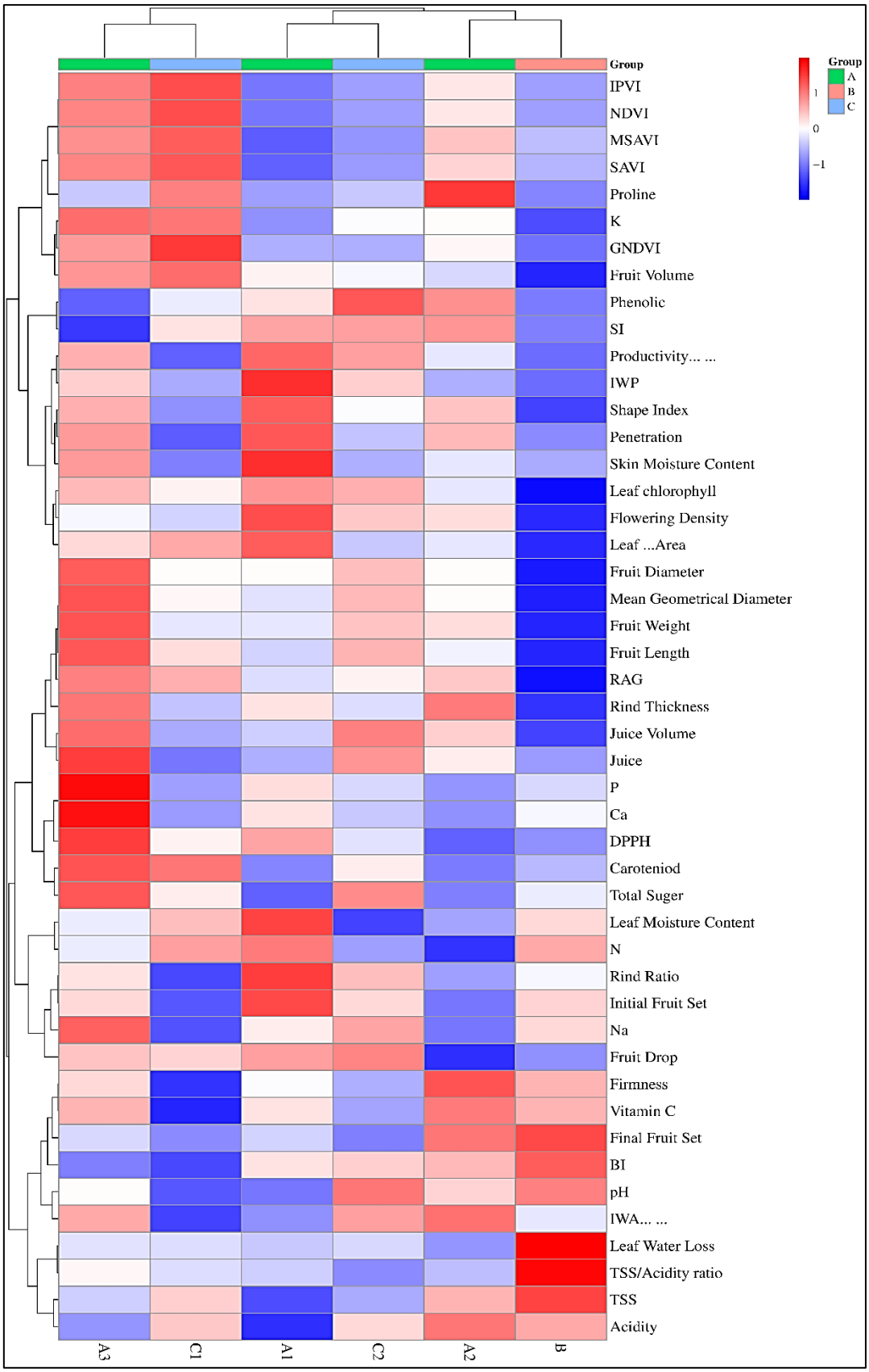

Abbreviations: Brightness Index (BI), Modified Soil Adjusted Vegetation Index (MSAVI), Soil Adjusted Vegetation Index (SAVI), Normalized Difference Vegetation Index (NDVI), Green Normalized Difference Vegetation Index (GNDVI), Infrared Percentage Vegetation Index (IPVI), Salinity Index (SI), Irrigation Water Applied (IWA), and Irrigation Water Productivity (IWP).

Fig. 9. Dendrogram of two-way cluster analysis of differ microirrigation systems treatments.

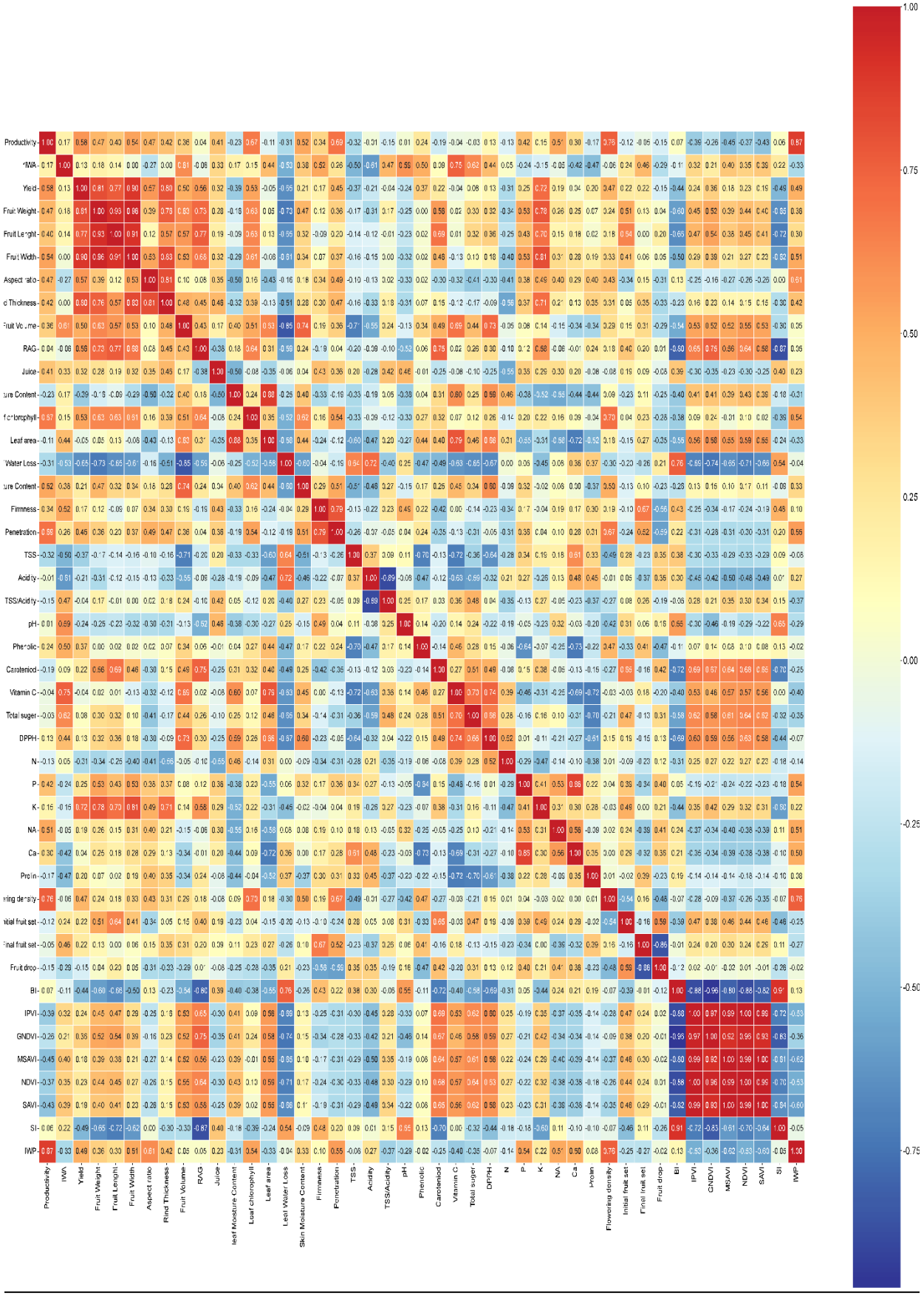

Fig. 10. Pearson's correlation matrix between vegetative growth parameters, quality parameters, remote sensing indices, and irrigation parameters of orange trees treated with different Microirrigation systems.

Table 15. Economic feasibility analysis for calculation of the net income of different microirrigation systems under orange trees.

Item		Costs (US$ y^{-1})					
		T-tape GR	Online dripper	Online PC dripper	Mist sprayers	RZWS	Bubbler
Fixed Costs (FC)	Administrative expenses	65.83	66.67	88.85	233.53	233.53	61.86
	Annual consumption 10% (without land rent)	6.58	6.67	8.89	23.35	23.35	6.19
	Rent (on season)	1190.00	1190.00	1190.00	1190.00	1190.00	1190.00
Total FC		**1262.41**	**1263.34**	**1287.74**	**1446.88**	**1446.88**	**1258.05**
Variable Costs (VC)	Irrigation	9.01	9.01	9.01	3.75	3.75	9.01
	Seedlings	150.00	150.00	150.00	150.00	150.00	150.00
	Fertilizers	952.00	952.00	952.00	952.00	952.00	952.00
	Pesticides	190.40	190.40	190.40	190.40	190.40	190.40
	Harvesting	88.84	107.85	89.98	124.88	123.12	133.17
	Maintenance (2.2-7.4% FC)	60.60	60.64	61.81	69.45	69.45	60.39
Total VC		**1450.84**	**1469.90**	**1453.20**	**1490.48**	**1488.72**	**1494.97**
Total cost (TC)		**2713.26**	**2733.24**	**2740.93**	**2937.36**	**2935.60**	**2753.02**
Total revenue (TR)	Yield (ton ha^{-1})	27.53	22.29	25.45	18.60	18.36	25.81
	Price (400 US$ ton^{-1})	11010.0	8916.0	10178.0	7438.0	7344.0	10322.0
Net farm income (NFI) = TR - TC		**8296.74**	**6182.76**	**7437.07**	**4500.64**	**4408.40**	**7568.98**

4. Discussions

4.1. The validity of sustainable management of saline irrigation water under different microirrigation systems

Recent research initiatives focusing on saline water have largely concentrated on traditional irrigation methods, particularly surface flooding, which often leads to excessive irrigation practices. However, there has been a notable transition towards more efficient irrigation techniques such as sprinkler and drip systems in recent years. The water quality limitations associated with these advanced systems differ significantly from those of conventional methods. To facilitate this transition, it is essential to gather information regarding the salinity, sodicity, and toxicity thresholds for various crops and horticultural species, alongside the establishment of crop-water production functions. The insights gained from this data can be instrumental in refining existing guidelines that advocate for the use of low-quality water in irrigation. Furthermore, the advent of smart irrigation technologies equipped with sensors and controllers allows for precise application of water, optimizing both the quantity and timing necessary for optimal plant growth. The effective implementation of these technologies is expected to enhance the sustainability of irrigation practices utilizing saline water.

The development of fruit trees in saline environments is significantly influenced by the irrigation technique employed, as well as its interaction with the quantity and distribution of rainfall at the location. The volume of saline irrigation water, which correlates with the chosen irrigation method and the rainfall received during the growing season, plays a crucial role in maintaining salt balance. Effective water productivity is greatly improved through precise scheduling, which ensures that the optimal amount of water is delivered to the fruit trees at the appropriate time and in the correct manner. This precision has encouraged farmers globally to implement micro-irrigation systems, such as

drip and sprinkler irrigation. Notably, drip irrigation has made substantial advancements for both vegetables and fruit trees, as it allows for the direct application of water and nutrients to the root zone, promoting efficient and judicious use of resources in fruit orchards.

Research by Hoffman and Shannon (2007) and Hanson (2012) has shed light on the fundamental principles and strategies for utilizing saline waters through drip irrigation systems. Enhanced water management and leaching are achieved in proximity to the emitters, where salt concentrations are kept only marginally above that of the irrigation water. By encouraging the majority of their root systems to develop near the emitters, plants can better withstand the use of irrigation waters with higher salinity. Hanson et al. (2009) illustrated that the wetting pattern surrounding the emitters leads to increased leaching fractions and reduced salinity levels compared to other irrigation methods for the same volume of water applied. These researchers characterized the localized leaching fraction as the actual leaching fraction that reflects the local root zone near the drip line. However, it is important to exercise caution when using drip irrigation in arid regions during the initial rainfall events, as these can potentially displace salts from the soil surface or the edges of the wetted area into the root zone, causing harm. It is essential to maintain irrigation practices even after the onset of rainfall, as interruptions in irrigation can lead to salinity-related damage, which is often evidenced by defoliation in various orchards. In our field experiments, we implemented strategies that involved determining the LF value and applying it alongside irrigation water. Continuous irrigation during rainfall events was crucial to prevent the salinity diffusion cone from encroaching upon the root zone.

The use of micro-sprinklers and mist sprayers has been shown to be more efficient than traditional flooding methods, as they enhance the microclimate by lowering temperatures and increasing humidity, thereby promoting optimal tree growth. Conversely, overhead sprinklers can result in the partial or complete wetting of foliage during the summer months, which contributes to a cooler microclimate and elevated humidity levels, ultimately fostering improved growth and yield. However, the wetting of foliage by sprinkler irrigation, whether partial or full, may lead to damage in the leaves of trees situated beneath the canopy. Symptoms of such damage, often resulting from direct exposure to saline water and the toxic accumulation of chloride (Cl) and sodium (Na), include burned, necrotic, or desiccated leaf tips, as noted by Maas (1990). Notably, the concentration of Cl and Na in the lower leaves of grapefruit and oranges was found to be nearly four times greater than that in the upper leaves. The thresholds for Na and Cl concentrations in irrigation water that can induce foliar injury through saline sprinkling are identified as < 0.5 and 0.5 – 1.0 dS m^{-1} for citrus, respectively. Furthermore, higher salt accumulations are observed with intermittent wetting compared to continuous wetting, and daytime sprinkling is more detrimental than nighttime applications. The rate of evaporation exacerbates the concentration of salts, leading to increased damage, as highlighted by Qadir et al. (2023). At the outset of the experiment, it became clear that the initial setup included a micro-sprinkler system. However, the unusually high levels of sodium and chlorine in the irrigation water, which measured 4.97 and 5.16 dS m^{-1} respectively, led to the burning of orange leaves, particularly when using the micro-sprinkler system. The detrimental impact of the salinity in the irrigation water was more pronounced with micro-sprinklers, prompting the decision to eliminate this irrigation method and proceed with the experiment utilizing mist sprayers, allowing for a comparative analysis with other micro-irrigation systems.

4.2. Effects of management strategy of saline irrigation water on salts distribution patterns

In their study, Paiva et al. (2023) investigated the effects of saline irrigation on the characteristics of sour passion fruit genotypes in the semi-arid region of Paraíba, Brazil. The research involved five different levels of electrical conductivity of irrigation water (EC_w) ranging from 0.3 to 3.5 dS m^{-1}, alongside three distinct genotypes of sour passion fruit. The findings indicated that an increase in the electrical conductivity of the irrigation water adversely impacted the physiological traits of the sour passion fruit, particularly noted at 154 days post-transplantation. The study revealed significant variations in the tolerance of different sour passion fruit genotypes to saline irrigation. Notably, the percentage of cell membrane damage escalated with higher electrical conductivity, especially at 3.5 dS m^{-1}. Interestingly, the genotype '*BRS Sol do Cerrado*' exhibited enhanced synthesis of photosynthetic pigments under the same saline conditions, achieving peak values of 1439.23 g mL^{-1} for chlorophyll a, 290.96 g mL^{-1} for chlorophyll b, 1730.19 g mL^{-1} for total chlorophyll, and 365.84 g mL^{-1} for carotenoids. These results align with previous findings by Paiva et al. (2023), which demonstrated that the Valencia orange tree displayed considerable salinity tolerance, particularly with drip irrigation, as evidenced by chlorophyll and carotenoid levels. The online PC

dripper recorded the highest leaf chlorophyll concentration of 71.575 SPAD during the second growing season, while the Mist sprayer yielded the lowest at 46.328 SPAD. Additionally, the online PC dripper achieved a maximum carotenoid concentration of 0.278 g 100 g^{-1} in the first growing season, contrasting with the online dripper's minimum of 0.148 g 100 g^{-1} in the second growing season, all under irrigation water salinity of 7.01 dS m^{-1}.

4.3. Soil moisture and salt distribution pattern under different microirrigation systems

Soil salinization plays a crucial role in the deterioration of soil quality and the reduction of fertility. This issue is primarily driven by the use of poor-quality irrigation water and inadequate irrigation management practices. The problem is intensified by the use of water that contains high levels of salinity (Wada et al., 2016, Pandit et al., 2020). The combined effects of salinization in both soil and water negatively impact plant growth, resulting in significant economic losses in agricultural production (Mirlas, 2012). Studies on soil moisture and salt distribution under Valencia orange trees indicate that without proper irrigation strategies, there is a tendency for increased soil salinity and ongoing soil fertility decline. The salinization process is characterized by the buildup of salts in the upper root zone of the trees after the summer irrigation season. During irrigation, soluble salts are quickly washed down to deeper soil layers and spread laterally around the dripper within the top 20–30 cm of the soil profile. However, within approximately 24 hours after irrigation, salinity levels in the soil begin to rise again. The soil experiences drying, which leads to salt accumulation at the surface due to evapotranspiration.

In their study, Mirlas et al. (2020) employed a variety of methodological strategies, including the monitoring of soil salinity, execution of field trials, application of remote sensing technologies, and modeling the dynamics of saline water movement within unsaturated soil profiles. Their assessment focused on the salinization processes affecting chalky soil irrigated through drip systems with water of differing quality. Specifically, when utilizing water with a dissolved salt concentration of 3.13 dS m^{-1}, the researchers observed a notable accumulation of salts in the upper root zone of the trees. The modeling results revealed a considerable risk of soil salinization associated with the use of saline water, whereas the application of potable water was effective in alleviating salinization issues. These findings corroborate our own observations, which indicated that T-tape (GR) drippers resulted in the most significant fluctuation in salt concentration, decreasing from 1900 ppm to 800 ppm post-irrigation. This was succeeded by the online PC drippers, which lowered salt concentration from 2100 ppm to 1100 ppm, achieving a reduction of 1000 ppm under comparable conditions. Conversely, the Mist sprayers system demonstrated the least effect on salt concentration, with a reduction from 1500 ppm to 1300 ppm, leading to a decrease of 200 ppm at a horizontal distance of 1 meter and a depth of 0.50 m (Fig. 4).

4.4. Effects of water and salt stresses on potential yield and fruit characteristics

Burt and Isbell (2005) emphasized that although drip irrigation may demonstrate irregular water distribution at a micro scale, it generally achieves a consistent application at macro levels and over extended periods, thereby offering compelling prospects for its application with saline water. Various research studies have indicated improvements in yield and water use efficiency, as well as enhancements in crop size and quality when saline irrigation is employed. A recent meta-analysis conducted by Du et al. (2023) revealed that soil salinity levels in the root zone decreased by 37.1%, 30.3%, and 19.7% under drip irrigation compared to flooding irrigation, with the electrical conductivity of irrigation water (EC_{iw}) ranging from 2–10, 0.7–2, and 0–0.7 dS m^{-1}, respectively. This investigation achieved a reduction in soil salinity of approximately 1100 ppm at a horizontal distance of 1 meter from the tree and a depth of 0.50 meters under T-tape (GR), which also yielded the highest production of 27.51 ton ha^{-1} and 27.54 ton ha^{-1} in the first and second growing seasons, respectively, followed by the Bubbler system, which matched this yield. Conversely, the Mist sprayer treatment yielded the least at 19.10 ton ha^{-1} (Table 9).

Furthermore, salt stress resulted in a significant increase in proline content in the leaves of the affected plants, with the online dripper treatment exhibiting the highest proline levels of 59.547 mg 100 g^{-1} and 49.189 mg 100 g^{-1} in the first and second growing seasons, respectively. In contrast, the T-tape (GR) recorded the lowest proline content of 16.095 mg 100 g^{-1} during the second growing season (Table 14), with peak levels observed in the summer, coinciding with the lowest soil moisture and leaf water potential. The accumulation of proline was found to correlate directly with the duration of salt stress, corroborating the findings of Ashraf et al. (2008) and Shaheen et al. (2011), which indicated that proline levels significantly increase in higher plants in response to environmental stress.

4.5. The differential effects of irrigation amount on physicochemical properties of root zone soil

Irrigation plays a crucial role in both meeting the physiological growth requirements of fruit trees and enhancing the soil's structure, temperature, and moisture levels, thus fostering a more conducive environment for root development (Li et al., 2023). Research indicates a strong relationship between root growth and soil moisture, with inadequate deep soil moisture identified as a significant constraint on root development in fruit trees (Du et al., 2017). This investigation highlighted the importance of accurately determining irrigation volumes, including leaching needs for various water application methods through different micro-irrigation systems. The study found that effective irrigation promotes the downward leaching of salts, which alleviates the adverse effects of deep soil sloughing and mechanical resistance caused by salinity, thereby facilitating the growth of deep root systems and increasing root density. Notably, the salt concentration reduction observed before and after irrigation with drip systems, particularly the T-tape (GR) dripper, was significant, decreasing from 1900 ppm to 800 ppm, which corresponds to a remarkable reduction of 1100 ppm at a horizontal distance of 1 meter from the tree and a depth of 0.50 meters. In contrast, other systems such as Mist sprayers, RZWS, and Bubblers did not yield comparable results in terms of salt flushing when compared to drip systems. The method and distribution of irrigation water directly influence the root zone soil environment, with this study revealing variations in soil water content at different depths and treatments across the irrigation systems. The T-tape (GR) dripper and online PC dripper emerged as the most effective systems, achieving a consistent moisture distribution and reaching a field capacity of 19% at least 1.5 meters from the tree. Conversely, moisture content significantly decreased under RZWS and Mist sprayers, despite the latter's method of delivering water in a rain-like manner, particularly during periods of elevated temperatures and increased wind speeds.

Irrigation serves dual purposes: it fulfills the standard physiological growth needs of fruit trees and modifies soil structure, temperature, and moisture, thereby creating a more favorable inter-root environment (Li et al., 2023). Root growth was found to strongly correlate with soil moisture conditions, with insufficient deep soil moisture being a major factor limiting root growth in fruit trees (Du et al., 2017). This study demonstrated that accurate determination of irrigation volume including leaching requirements for different water application techniques through diverse micro-irrigation systems can be attributed to the enhanced downward leaching of salts caused by irrigation, which mitigates the deep soil sloughing effect and mechanical resistance induced by salts, thereby promoting deep root system growth and root density, where the salt removal before and after irrigation under drip irrigation systems revealed that the T-tape (GR) dripper was particularly effective, reducing salt concentration from 1900 ppm to 800 ppm, resulting in a notable decrease of 1100 ppm at a horizontal distance of 1 meter from the tree and a depth of 0.50 meters, on the other hand, Mist sprayers, RZWS, and Bubblers didn't achieves the promising resutts related to salt flushing comparing with drip systems. The way and distribution of irrigation water applied regulates the root zone soil environment, with this study indicating differences in soil water content at depth and treatment across various irrigation systems, where the best systems that achieved a regular moisture distribution and reached the soil sector to the field capacity of 19% for a distance of not less than 1.5 meters from the tree were T-tape (GR) dripper and online PC dripper, while the moisture distribution varied between the different systems with a significant decrease in the moisture content under both RZWS and Mist sprayers, although Mist sprayer add water in the form of falling rain, while with the rise in temperature and increase in wind speed. The consistency of distribution diminishes while evaporation losses escalate, adversely impacting the soil's moisture levels.

The root systems of fruit trees primarily thrive in soil strata characterized by elevated moisture levels. By improving the water content in deeper soil layers, not only is drought stress in fruit trees alleviated (Wang et al., 2024), but the efficiency of water uptake by the primary root system is also enhanced. Factors such as electrical conductivity (EC) and pH, which are critical for enhancing the quality of root zone soil, are positively affected by increased moisture levels, as this facilitates the leaching of salts within the root zone, thereby effectively mitigating the detrimental impacts of salinity on the root system (Hou et al., 2022, Liu et al., 2023). Conversely, The leaching of salts from deeper soil layers is promoted by heightened moisture content in the root zone, resulting in a reduction of pH and creating a more conducive environment for the root systems of fruit trees. Consequently, augmenting the water content in the primary root zone regulates thermal capacity and establishes a more stable hydrothermal environment, which alleviates the negative effects of elevated temperatures during the mid- to late-growth stages, thus playing a crucial role in the root

system's adaptation to heat stress (Hou et al., 2022, Liu et al., 2023).

4.6. The effectiveness of remote sensing indicators in sustainable irrigation water management

The relationship between salinity levels and vegetation indices underscores the significance of certain indices in assessing plant health. Among the indices analyzed, the Normalized Difference Vegetation Index (NDVI) and Brightness Index (BI) exhibited the strongest correlations with salinity metrics, thereby validating their roles as key indicators of vegetation vitality and resilience to stress. In contrast, while GNDVI, IPVI, and MSAVI provide valuable insights into specific aspects of vegetation, their relatively weaker correlations limit their utility as independent indicators. This study highlights the importance of integrating advanced irrigation strategies with reliable vegetation indices to effectively tackle salinity issues and foster sustainable agricultural practices. The results demonstrate the pivotal function of modern microirrigation systems in mitigating salinity stress and preserving plant health. Notably, the online PC dripper irrigation system consistently achieved higher NDVI values compared to other systems, indicating its superior ability to reduce salinity stress and enhance vegetation health. In contrast, the T-tape (GR) system produced lower NDVI values, pointing to insufficient water distribution and ineffective salinity management.

This evidence emphasizes the critical role of precision irrigation technologies in alleviating the impacts of salinity and improving water use efficiency. BI and NDVI have been recognized as essential metrics for monitoring salinity stress, with their strong correlations to salinity indices offering vital insights into plant health and adaptive responses. Although indices such as GNDVI, SAVI, IPVI, and MSAVI provide supplementary information, their weaker correlations limit their effectiveness as standalone indicators of stress.

The results of this study advocate for the incorporation of sophisticated irrigation technologies alongside remote sensing techniques to enhance sustainable agricultural practices. By employing Normalized Difference Vegetation Index (NDVI) and Biomass Index (BI) for immediate evaluations, agricultural producers can optimize their irrigation methods to mitigate the impacts of salinity and ensure the enduring viability of their farming operations. Subsequent research should prioritize the development of predictive models and sensor-driven monitoring systems to further improve irrigation management approaches in saline environments.

5. Conclusions

The use of saline water with an electrical conductivity of 7.01 dS m^{-1} for irrigating Valencia orange trees has been shown to elevate soil salinity levels. This study indicates that the response of orange trees to salinity in field conditions is influenced not only by the salinity of the irrigation water but also by various environmental factors, including the type of micro-irrigation system employed, climatic conditions, the growth stage of the trees, and the characteristics of the soil. The results suggest that employing T-tape (GR) drippers and online PC drippers on sandy soils may mitigate the risk of soil salinization under the experimental conditions examined. Given that saline irrigation water is the only available resource in the region, its effective utilization is critical. The application of different micro-irrigation systems to address this challenge has yielded encouraging outcomes, enhancing sustainable irrigation water productivity, vegetative growth, and quality parameters, with average yields of 4.92 kg m^{-3} and 4.08 kg m^{-3} across both growing seasons.

This approach has illustrated that irrigation can produce a higher quantity of oranges per unit of water, underscoring the need for more efficient practices in the use of low-quality water resources. The integration of saline water irrigation with drip systems has proven beneficial in alleviating drought conditions, fostering vegetative growth and yield while upholding quality standards. Additionally, effective leaching in light-textured soils within an arid climate has successfully managed salt accumulation in the soil. Nevertheless, long-term studies are essential to assess the sustainability of this irrigation strategy.

Despite the recognized advantages of employing saline water resources for agricultural and soil enhancement, this knowledge has not been adequately disseminated among pertinent stakeholders, leading to a significant reluctance to implement it for irrigation. It is crucial to improve the communication of policy recommendations based on research outcomes to keep stakeholders well-informed. Furthermore, there is a pressing need to upgrade the competencies of existing staff and to integrate new expertise to strengthen the oversight and management of water quality.

Consent for publication:

All authors declare their consent for publication.

Author contribution:

The manuscript was edited and revised by all authors.

Conflicts of Interest:
The author declares no conflict of interest.

Acknowledgments:
The authors would like to express their thanks to the Faculty of Agriculture, Cairo University, and Higher Institute of Agricultural Cooperation for their support in this work.

References

Abd-Elgawad, M. M. 2021. The Mediterranean Fruit Fly (Diptera: Tephritidae), A Key Pest Of Citrus In Egypt. *Journal Of Integrated Pest Management,* 12**,** 28.

Al-Agele, H. A. 2020. Irrigation Innovations To Increase Efficiency And Sustainability.

Al-Shammary, A. A. G., Kouzani, A. Z., Kaynak, A., Khoo, S. Y., Norton, M. & Gates, W. 2018. Soil Bulk Density Estimation Methods: A Review. *Pedosphere,* 28**,** 581-596.

Alcaraz, M.-A. L. & Hormaza, J. I. 2021. Fruit Set In Avocado: Pollen Limitation, Pollen Load Size, And Selective Fruit Abortion. *Agronomy,* 11**,** 1603.

Alonso-Vázquez, P., Isola, A., Sc!Nchez-Arc)Valo, C. M., Cuartas-Uribe, B., Vincent-Vela, M. C. & C Lvarez-Blanco, S. 2025. Concentration Of Phenolic Compounds From An Orange Peel Waste Extract Using A Combination Of Ultrafiltration And Forward Osmosis. *Separation And Purification Technology,* 360**,** 131228.

Alshallash, K. S., Sharaf, M., Abdel-Aziz, H. F., Arif, M., Hamdy, A. E., Khalifa, S. M., Hassan, M. F., Abou Ghazala, M. M., Bondok, A. & Ibrahim, M. T. 2022. Postharvest Physiology And Biochemistry Of Valencia Orange After Coatings With Chitosan Nanoparticles As Edible For Green Mold Protection Under Room Storage Conditions. *Frontiers In Plant Science,* 13**,** 1034535.

Anyaegbu, C., Ibekwe, U., Odii, M., Ehirim, N., Chikezie, C., Ogbonna, S. & Chukwurah, V. 2020. Analysis Of Net Farm Income And Non-Farm Income Of Broiler Farmers Across Different Scale Of Production In Imo State, Nigeria. *Journal Of Agriculture And Food Sciences,* 18**,** 98-108.

Ashwell, G. 1957. Colorimetric Analysis Of Sugars.

Awad, A. E., Abuarab, M. E., Abdelraouf, R., Bakeer, G. A., El-Shawadfy, M. A. & Ragab, R. 2024. Improving Yield And Irrigation Water Productivity Of Green Beans Under Water Stress With Agricultural Solid Waste-Based Material Of Compacted Rice Straw As A Sustainable Organic Soil Mulch. *Irrigation Science***,** 1-26.

Batjes, N. H., Ribeiro, E. & Van Oostrum, A. 2020. Standardised Soil Profile Data To Support Global Mapping And Modelling (Wosis Snapshot 2019). *Earth System Science Data,* 12**,** 299-320.

Burt, C. M. & Isbell, B. 2005. Leaching Of Accumulated Soil Salinity Under Drip Irrigation. *Transactions Of The Asae,* 48**,** 2115-2121.

Chetto, O., Abbouch, B., Douaik, A., Talha, A. & Benyahia, H. 2025. Multivariate Analysis Of Phenotypic Diversity In Moroccan Orange Accessions (Citrus Sinensis L. Osbeck) From The El Menzeh Collection. *African And Mediterranean Agricultural Journal-Al Awamia***,** 31-44.

Chikankheni, A. T. 2023. *Investigation Into The Effects Of Deficit Irrigation On Potato Production In Dedza District-Malawi.* The University Of Zambia.

Christiansen, J. 1942. Irrigationirrigation By Sprinkling. California Agricultural Experiment Station Bulletin 670'. *Univ. California, Berkeley, Ca,* 4275.

Crippen, R. E. 1990. Calculating The Vegetation Index Faster. *Remote Sensing Of Environment,* 34**,** 71-73.

Daba, A. W. & Qureshi, A. S. 2021. Review Of Soil Salinity And Sodicity Challenges To Crop Production In The Lowland Irrigated Areas Of Ethiopia And Its Management Strategies. *Land,* 10**,** 1377.

Dewis, J. & Freitas, F. 1970. Physical And Chemical Methods Of Soil And Water Analysis.

Dinar, A. 2024. Challenges To Water Resource Management: The Role Of Economic And Modeling Approaches. *Water,* 16**,** 610.

Djaman, K., Ob, Owen, C. K., Smeal, D., Koudahe, K., West, M., Allen, S., Lombard, K. & Irmak, S. 2018. Crop Evapotranspiration, Irrigation Water Requirement And Water Productivity Of Maize From Meteorological Data Under Semiarid Climate. *Water,* 10**,** 405.

Domingues, A. R., Marcolini, C. D. M., Goncalves, C. H. D. S., Goncalves, L. S. A., Roberto, S. R. & Carlos, E. F. 2020. Fruit Ripening Development Of B. *Horticulturae,* 7**,** 3.

Du, S., Kang, S., Li, F. & Du, T. 2017. Water Use Efficiency Is Improved By Alternate Partial Root-Zone Irrigation Of Apple In Arid Northwest China. *Agricultural Water Management,* 179**,** 184-192.

Du, Y., Liu, X., Zhang, L. & Zhou, W. 2023. Drip Irrigation In Agricultural Saline-Alkali Land Controls Soil Salinity And Improves Crop Yield: Evidence From A Global Meta-Analysis. *Science Of The Total Environment,* 880**,** 163226.

Dubey, A. K., Rao, K., Kumar, S., Tamta, M., Dwivedi, S., Kumar, R. & Mishra, J. 2019. Disease Management In Major Field Crops. *Conservation Agriculture For Climate Resilient Farming & Doubling Farmersb*.

Elhag, M. 2016. Evaluation Of Different Soil Salinity Mapping Using Remote Sensing Techniques In Arid Ecosystems, Saudi Arabia. *Journal Of Sensors,* 2016**,** 7596175.

Elhag, M. & Bahrawi, J. A. 2017. Soil Salinity Mapping And Hydrological Drought Indices Assessment In Arid Environments Based On Remote Sensing Techniques. *Geoscientific Instrumentation, Methods And Data Systems,* 6**,** 149-158.

Elhosary, M. S., Elmetwalli, A., Derbala, A. & Elsayed, S. 2023. Image Analysis Technique For Evaluating The Quality Of Navel Orange Fruits. *Journal Of Sustainable Agricultural And Environmental Sciences,* 2**,** 100-109.

Elkot, A. F., Elrashidy, Z. A. A. & Gab Alla, M. M. M. 2023. Evaluation Of Eight Bread Wheat Cultivars For Soil Salinity Tolerance. *Egyptian Journal Of Agronomy,* 45**,** 157-170.

Erkmen, O. & Bozkurt, H. 2004. Quality Characteristics Of Retailed Sucuk (Turkish Dry-Fermented Sausage). *Food Technology And Biotechnology,* 42**,** 63-69.

Esa, E. 2018. Copernicus Open Access Hub. Esa (European Spatial Agency).

Escadafal, R. 1989. Remote Sensing Of Arid Soil Surface Color With Landsat Thematic Mapper. *Advances In Space Research,* 9**,** 159-163.

Ferreira, A. N., Rolim, J. O., Paredes, P. & Cameira, M. D. R. R. 2023. Methodologies For Water Accounting At The Collective Irrigation System Scale Aiming At Optimizing Water Productivity. *Agronomy,* 13**,** 1938.

Francob, Padilla, Y. G., C Lvarez, S., Calatayud, C. N., Colmenerob, Gc3mezb, Hernc!Ndez, J. A., Martc-Nezb, Penella, C. & Pc)Rezb 2025. Advancements In Waterb. *Physiologia Plantarum,* 177**,** E70332.

Gascon, F., Bouzinac, C., Thepaut, O., Jung, M., Francesconi, B., Louis, J., Lonjou, V., Lafrance, B., Massera, S. & Gaudel-Vacaresse, A. 2017. Copernicus Sentinel-2a Calibration And Products Validation Status. *Remote Sensing,* 9**,** 584.

Gorji, T., Sertel, E. & Tanik, A. 2017. Monitoring Soil Salinity Via Remote Sensing Technology Under Data Scarce Conditions: A Case Study From Turkey. *Ecological Indicators,* 74**,** 384-391.

Gunny, A. A. N., Gopinath, S. C., Ali, A., Wongs-Aree, C. & Salleh, N. H. M. 2024. Challenges Of Postharvest Water Loss In Fruits: Mechanisms, Influencing Factors, And Effective Control Strategies–A Comprehensive Review. *Journal Of Agriculture And Food Research***,** 101249.

Handel, P. 1968. Instabilities And Turbulence In Semiconductors. *Physica Status Solidi (B),* 29**,** 299-306.

Hanson, B. R. 2012. Drip Irrigation And Salinity. *Agricultural Salinity Assessment And Management.*

Hanson, B. R., May, D. E., Simunek, J., Hopmans, J. W. & Hutmacher, R. B. 2009. Drip Irrigation Provides The Salinity Control Needed For Profitable Irrigation Of Tomatoes In The San Joaquin Valley. *California Agriculture,* 63.

Hoffman, G. J. & Shannon, M. C. 2007. 4. Salinity. *Developments In Agricultural Engineering.* Elsevier.

Hou, X., Xiang, Y., Fan, J., Zhang, F., Hu, W., Yan, F., Xiao, C., Li, Y., Cheng, H. & Li, Z. 2022. Spatial Distribution And Variability Of Soil Salinity In Film-Mulched Cotton Fields Under Various Drip Irrigation Regimes In Southern Xinjiang Of China. *Soil And Tillage Research,* 223**,** 105470.

Huang, S., Tang, L., Hupy, J. P., Wang, Y. & Shao, G. 2021. A Commentary Review On The Use Of Normalized Difference Vegetation Index (Ndvi) In The Era Of Popular Remote Sensing. *Journal Of Forestry Research,* 32**,** 1-6.

Ibrahim, A. A. 2022. Effect Of Soil Salinity Improvers On Cotton Productivity On Land Reclamation. *Egyptian Journal Of Agronomy,* 44**,** 19-31.

Ibrahim, M. M. & Gad, M. M. 2015. The Relationship Between Harvest Date And Storage Life Of Washington Navel Orange Fruits. *Middle East J. Appl. Sci,* 5**,** 1247-1256.

Inácio, M., Das, M., Barceló, D. & Pereira, P. 2023. Frameworks For Mapping Lake Ecosystem Services. An Example From Lithuania. *Methodsx,* 10**,** 102015.

Isdory, D., Massawe, B. & Msanya, B. 2021. Predicting Soil Ece Based On Values Of Ec1: 2.5 As An Indicator Of Soil Salinity At Magozi Irrigation Scheme, Iringa, Tanzania. *Tanzania Journal Of Agricultural Sciences,* 20**,** 63-71.

Jackson, M. 1973. Soil Chemical Analysis, Pentice Hall Of India Pvt. *Ltd., New Delhi, India,* 498**,** 151-154.

James, L. G. 1988. *Principles Of Farm Irrigation Systems Design*.

Jindo, K., Kozan, O., Iseki, K., Maestrini, B., Van Evert, F. K., Wubengeda, Y., Arai, E., Shimabukuro, Y. E., Sawada, Y. & Kempenaar, C. 2021. Potential Utilization Of Satellite Remote Sensing For Field-Based Agricultural Studies. *Chemical And Biological Technologies In Agriculture,* 8**,** 1-16.

Junsomboon, J. & Jakmunee, J. 2020. New Extraction Procedure And Differential Pulse Voltammetric Method For Determination Of Water Soluble Chromium (Vi) Content In Portland Cement Products. *Chiang Mai Journal Of Science,* 47**,** 147-159.

Karmeli, D. & Keller, J. 1975. Trickle Irrigation Design. Rain Bird Sprinkler Manufacturing Corporation California.

Kasapidou, E., Mitlianga, P., Basdagianni, Z., Papatzimos, G., Mai, S., Barampouti, E. M., Papadopoulos, V. & Karatzia, M.-A. 2025. Orange Peel Feed Ingredient In Lactating Ewes: Effect On Yoghurt Chemical Composition, Fatty Acid Profile, Antioxidant Activity, Physicochemical Properties, And Sensory Quality. *Applied Sciences,* 15**,** 3641.

Keller, J. & Bliesner, R. D. 1990. Layout Of Set Sprinkler Systems. *Sprinkle And Trickle Irrigation.* Springer.

Khan, N., Fahad, S., Naushad, M. & Faisal, S. 2020. Pomegrantes Economics And Medicinal Aspects In The World. *Available At Ssrn 3597891*.

Klute, A. & Dirksen, C. 1986. Hydraulic Conductivity And Diffusivity: Laboratory Methods. *Methods Of Soil Analysis: Part 1 Physical And Mineralogical Methods,* 5**,** 687-734.

Kumar, R., Sharma, M. & Singh, S. K. 2018. Integrated Approach To Control Of Fruit Drop And Improvement Of Yield In Kinnow (Citrus Nobilis X Citrus Deliciosa). *Walailak Journal Of Science And Technology (Wjst),* 15**,** 819-829.

Lamm, F. R., Colaizzi, P. D., Sorensen, R. B., Bordovsky, J. P., Dougherty, M., Balkcom, K., Zaccaria, D., Bali, K. M., Rudnick, D. R. & Peters, R. T. 2021. A 2020 Vision Of Subsurface Drip Irrigation In The Us. *Transactions Of The Asabe,* 64**,** 1319-1343.

Li, Z., Li, W., Wang, J., Zhang, J. & Wang, Z. 2023. Drip Irrigation Shapes The Soil Bacterial Communities And Enhances Jujube Yield By Regulating The Soil Moisture Content And Nutrient Levels. *Agricultural Water Management,* 289**,** 108563.

Lillesand, T. & Kiefer, R. 2004. Chipman, Jw 2004. *Remote Sensing And Image Interpretation. John Wiley &Sons, New York, Usa,* 31.

Liu, X., Yan, F., Wu, L., Zhang, F., Yin, F., Abdelghany, A. E., Fan, J., Xiao, C., Li, J. & Li, Z. 2023. Leaching Amount And Timing Modified The Ionic Composition Of Saline-Alkaline Soil And Increased Seed Cotton Yield Under Mulched Drip Irrigation. *Field Crops Research,* 299**,** 108988.

Maas, E. 1990. Crop Salt Tolerance. *Agricultural Salinity Assessment And Management Manual***,** 262-304.

Mansey, M. T., El-Zaher, A., Helmy, M., Hamed, H. H. & Abd Elrahman, A. E. M. 2021. Diagnosis And Remedy Of Boron Deficiency In Valencia Orange Trees Under Two Different Sites Conditions. *Egyptian Journal Of Chemistry,* 64**,** 6993-6999.

Mansour, H. 2025. Enhancing Maize Productivity Through Aquacrop Modeling Under Modern Irrigation Systems And Drought Stress Conditions. *Egyptian Journal Of Agronomy,* 47**,** 55-71.

Martínez, F., Oliveira, J. A., Calvete, E. O. & Palencia, P. 2017. Influence Of Growth Medium On Yield, Quality Indexes And Spad Values In Strawberry Plants. *Scientia Horticulturae,* 217**,** 17-27.

Mccready, R., Guggolz, J., Silviera, V. & Owens, H. 1950. Determination Of Starch And Amylose In Vegetables. *Analytical Chemistry,* 22**,** 1156-1158.

Mckie, V. A. & McCleary, B. V. 2016. A Novel And Rapid Colorimetric Method For Measuring Total Phosphorus And Phytic Acid In Foods And Animal Feeds. *Journal Of Aoac International,* 99**,** 738-743.

Mengu, G. P., Pouyafard, N., Kaya, Ü. & Akkuzu, E. 2024. Examination Of Temporal Variation In The Physiological Parameters Of Olive Trees In Various Deficit Irrigation Strategies. *Journal Of Irrigation And Drainage Engineering,* 150**,** 04024011.

Miller, G. L. 1959. Use Of Dinitrosalicylic Acid Reagent For Determination Of Reducing Sugar. *Analytical Chemistry,* 31**,** 426-428.

Minhas, P., Ramos, T. B., Ben-Gal, A. & Pereira, L. S. 2020. Coping With Salinity In Irrigated Agriculture: Crop Evapotranspiration And Water Management Issues. *Agricultural Water Management,* 227**,** 105832.

Mirlas, V. 2012. Assessing Soil Salinity Hazard In Cultivated Areas Using Modflow Model And Gis Tools: A Case Study From The Jezre'el Valley, Israel. *Agricultural Water Management,* 109**,** 144-154.

Mirlas, V., Anker, Y., Aizenkod, A. & Goldshleger, N. 2020. Soil Salinization Risk Assessment Owing To Poor Water Quality Drip Irrigation: A Case Study From An Olive Plantation At The Arid To Semi-Arid Beit She'an Valley, Israel, Geoscientific Model Development Discussions. *Doi,* 10**,** 1-31.

Mompremier, R., Her, Y., Hoogenboom, G., Migliaccio, K., Muñoz-Carpena, R., Brym, Z., Colbert, R. & Jeune, W. 2021. Modeling The Response Of Dry Bean Yield To Irrigation Water Availability Controlled By Watershed Hydrology. *Agricultural Water Management,* 243**,** 106429.

Mossad, A., Farina, V. & Lo Bianco, R. 2020. Fruit Yield And Quality Of B. *Agronomy,* 10**,** 164.

Moumouni Koala, A. H., Somc), K., Palc), E., Sc)Rc)Mc), A., Belem, J. R. M. & Nacro, M. 2013. Evaluation Of Eight Orange Fleshed Sweetpotato (Ofsp) Varieties For Their Total Antioxidant, Total Carotenoid And Polyphenolic Contents. *Evaluation,* 3**,** 67-73.

Moursy, M. A. M., Elfetyany, M., Meleha, A. M. I. & El-Bialy, M. A. 2023. Productivity And Profitability Of Modern Irrigation Methods Through The Application Of On-Farm Drip Irrigation On Some Crops In The Northern Nile Delta Of Egypt. *Alexandria Engineering Journal,* 62**,** 349-356.

Napitupulu, T. S., Nadhirah, A., Marseva, A. D., Kinanti, L. A. B. & Ferinta, A. Determining Consumer Preferences For Orange Attributes: A Conjoint Analysis Approach At The Teaching Factory, Politeknik Negeri Jember. Iop Conference Series: Earth And Environmental Science, 2025. Iop Publishing, 012055.

Nnamdi, U. B., Onyejiuwa, C. T. & Ogbuke, C. R. 2020. Review Of Orange Juice Extractor Machines. *Advances In Science, Technology And Engineering Systems Journal,* 5**,** 485-492.

Okal, H. A., Ngetich, F. K. & Okeyo, J. M. 2020. Spatio-Temporal Characterisation Of Droughts Using Selected Indices In Upper Tana River Watershed, Kenya. *Scientific African,* 7**,** E00275.

Olamide, F. O., Olalekan, B. A., Tobi, S. U., Adeyemi, M. A., Julius, J. O. & Oluwaseyi, F. K. 2022. Fundamentals Of Irrigation Methods And Their Impact On Crop Production. *Irrigation And Drainage-Recent Advances.* Intechopen.

Omokolo Ndoumou, D., Tsala Ndzomo, G. & Djocgoue, P. 1996. Changes In Carbohydrate, Amino Acid And Phenol Contents In Cocoa Pods Fromthree Clones After Infection With Phytophthora Megakarya Bra. And Grif. *Annals Of Botany,* 77**,** 153-158.

Ouda, S. 2020a. Accurate Estimation Of Crop Coefficients For Better Irrigation Water Management In Egypt. *Technological And Modern Irrigation Environment In Egypt.* Springer.

Ouda, S. 2020b. Accurate Estimation Of Crop Coefficients For Better Irrigation Water Management In Egypt. *Technological And Modern Irrigation Environment In Egypt: Best Management Practices & Evaluation.* Springer.

Paiva, F. J. D. S., Lima, G. S. D., Lima, V. L. A. D., Souza, W. B. B. D., Soares, L. A. D. A., Torres, R. A. F., Gheyi, H. R., Silva, L. D. A., Sá, F. V. D. S. & Sá, V. K. N. O. D. 2023. The Effects Of Irrigation Water Salinity On The Synthesis Of Photosynthetic Pigments, Gas Exchange, And Photochemical Efficiency Of Sour Passion Fruit Genotypes. *Plants,* 12**,** 3894.

Pandit, R., Parrotta, J. A., Chaudhary, A. K., Karlen, D. L., Vieira, D. L. M., Anker, Y., Chen, R., Morris, J., Harris, J. & Ntshotsho, P. 2020. A Framework To Evaluate Land Degradation And Restoration Responses For Improved Planning And Decision-Making. *Ecosystems And People,* 16**,** 1-18.

Pibars, S. K., Mansour, H., Koheal, H. K. & Imam, H. M. 2025. Sustainable Water Management Using Soil Mulching And Drip Irrigation Strategies For Faba Bean Production. *Egyptian Journal Of Agronomy,* 47**,** 825-833.

Qadir, M., Drechsel, P., Salcedo, F. P., Robles, L. P., Ben-Gal, A. & Grattan, S. R. 2023. Chemical Risks And Risk Management Measures Of Relevance To Crop Production With Special Consideration Of Salinity.

Qi, J., Chehbouni, A., Huete, A. R., Kerr, Y. H. & Sorooshian, S. 1994. A Modified Soil Adjusted Vegetation Index. *Remote Sensing Of Environment,* 48**,** 119-126.

Richards, L. A. 1954. *Diagnosis And Improvement Of Saline And Alkali Soils*, Us Government Printing Office.

Rouse, J. H., Shaw, J. A., Lawrence, R. L., Lewicki, J. L., Dobeck, L. M., Repasky, K. S. & Spangler, L. H. 2010. Multi-Spectral Imaging Of Vegetation For Detecting Co 2 Leaking From Underground. *Environmental Earth Sciences,* 60**,** 313-323.

Saad, A. M., Soussa, H., Ramadan, A. & Abdelsalheen, M. 2025. Performance Of Remote Sensing In Scheduling Irrigation: A Review. *Egyptian Journal Of Agronomy,* 47**,** 629-644.

Salcedo, F. P., Cutillas, P. P., Cabañero, J. J. A. & Vivaldi, A. G. 2022. Use Of Remote Sensing To Evaluate The Effects Of Environmental Factors On Soil Salinity In A Semi-Arid Area. *Science Of The Total Environment,* 815**,** 152524.

Salemi, H., Toomanian, N., Jalali, A., Nikouei, A., Khodagholi, M. & Rezaei, M. 2020. Determination Of Net Water Requirement Of Crops And Gardens In Order To Optimize The Management Of Water Demand In Agricultural Sector. *Standing Up To Climate Change: Creating Prospects For A Sustainable Future In Rural Iran.* Springer.

Sanaa, M. M. & Abd El-Rahman, G. 2023. Effects Of Exogenous Application Of Glycine Betaine And Proline On Productivity Of Valencia Orange Trees Grown In A Saline Soil. *Hortic. Res. J,* 1**,** 171-84.

Sefrin, O., Riese, F. M. & Keller, S. 2020. Deep Learning For Land Cover Change Detection. *Remote Sensing,* 13**,** 78.

Shaheen, M., Egazi, A. & Hmmam, I. 2011. Effect Of Salinity Treatments On Vegetative Characteristics And Leaves Chemical Content Of Transplants Of Five Olive Cultivars. *Journal Of Horticultural Science And Ornamental Plants,* 3**,** 143-151.

Shamili, M. 2019. The Estimation Of Mango Fruit Total Soluble Solids Using Image Processing Technique. *Scientia Horticulturae,* 249**,** 383-389.

Sishodia, R. P., Ray, R. L. & Singh, S. K. 2020. Applications Of Remote Sensing In Precision Agriculture: A Review. *Remote Sensing,* 12**,** 3136.

Stavi, I., Thevs, N. & Priori, S. 2021. Soil Salinity And Sodicity In Drylands: A Review Of Causes, Effects, Monitoring, And Restoration Measures. *Frontiers In Environmental Science,* 9**,** 712831.

Stern, R. 1991. Costat-Statutical Software. California: Cohort Software (1989), Pp. 302, $76.00. *Experimental Agriculture, 27, 87-87.*

Tiencheu, B., Nji, D. N., Achidi, A. U., Egbe, A. C., Tenyang, N., Ngongang, E. F. T., Djikeng, F. T. & Fossi, B. T. 2021. Nutritional, Sensory, Physico-Chemical, Phytochemical, Microbiological And Shelf-Life Studies Of Natural Fruit Juice Formulated From Orange (Citrus Sinensis), Lemon (Citrus Limon), Honey And Ginger (Zingiber Officinale). Heliyon, 7.

Tshazi, Z. 2022. Estimating Estuarine Suspended Sediment Concentration Through Spectral Indices And Band Ratios Derived From Sentinel-2 Data: A Case Of Umzimvubu Estuary, South Africa.

Velez, S., Martínez-Peña, R. & Castrillo, D. 2023. Beyond Vegetation: A Review Unveiling Additional Insights Into Agriculture And Forestry Through The Application Of Vegetation Indices. *J,* 6**,** 421-436.

Viña, A. & Gitelson, A. A. 2010. Sensitivity To Foliar Anthocyanin Content Of Vegetation Indices Using Green Reflectance. *Ieee Geoscience And Remote Sensing Letters,* 8**,** 464-468.

Vuong, Q. V., Hirun, S., Chuen, T. L., Goldsmith, C. D., Bowyer, M. C., Chalmers, A. C., Phillips, P. A. & Scarlett, C. J. 2014. Physicochemical Composition, Antioxidant And Anti-Proliferative Capacity Of A Lilly Pilly (Syzygium Paniculatum) Extract. *Journal Of Herbal Medicine,* 4**,** 134-140.

Wada, Y., Flörke, M., Hanasaki, N., Eisner, S., Fischer, G., Tramberend, S., Satoh, Y., Van Vliet, M., Yillia, P. & Ringler, C. 2016. Modeling Global Water Use For The 21st Century: The Water Futures And Solutions (Wfas) Initiative And Its Approaches. *Geoscientific Model Development,* 9**,** 175-222.

Wang, J., He, X., Gong, P., Heng, T., Zhao, D., Wang, C., Chen, Q., Wei, J., Lin, P. & Yang, G. 2024. Response Of Fragrant Pear Quality And Water Productivity To Lateral Depth And Irrigation Amount. *Agricultural Water Management,* 292**,** 108652.

Yan, K., Gao, S., Yan, G., Ma, X., Chen, X., Zhu, P., Li, J., Gao, S., Gastellu-Etchegorry, J.-P. & Myneni, R. B. 2025. A Global Systematic Review Of The Remote Sensing Vegetation Indices. *International Journal Of Applied Earth Observation And Geoinformation,* 139**,** 104560.

Zeng, Y., Hao, D., Huete, A., Dechant, B., Berry, J., Chen, J. M., Joiner, J., Frankenberg, C., Bond-Lamberty, B. & Ryu, Y. 2022. Optical Vegetation Indices For Monitoring Terrestrial Ecosystems Globally. *Nature Reviews Earth & Environment,* 3**,** 477-493.

Zieg, J. & Zawada, D. G. 2021. Improving Esri Arcgis Performance Of Coastal And Seafloor Analyses With The Python Multiprocessing Module. *Journal Of Coastal Research,* 37**,** 1288-1293.